14. THE PETROLOGY OF THE BASALTS, LEG 26 [1]

D. R. C. Kempe, British Museum (Natural History), London, England

ABSTRACT

Basalt, assumed to be conformable basement, was cored from six out of nine holes on Leg 26. From Site 250 olivine-rich, low potash basalt with calc-alkaline affinities was drilled, while Site 251 yielded typical spreading-ridge ocean-floor tholeiite. Sites 253 and 254 (Ninetyeast Ridge) produced altered basalts of varying types: the presumed basement from Site 253 is picritic while a scoriaceous flow from the overlying ash sequence is quartz-normative. The Wharton Basin sites (256 and 257) yielded fairly fresh quartz-normative tholeiite of widely differing compositions and phase chemistry.

The texture of the basalts varies widely from glassy and variolitic to hyalo-ophitic and subophitic. Only Sites 253 (basement) and 257 basalts are porphyritic. Basalts from Site 257 and a few others are highly vesicular, the vesicles being filled with celadonite, smectite, and calcite. Celadonite also forms veins and locally replaces all the pre-existing minerals, including plagioclase.

The phase mineralogy (pyroxenes and plagioclases; all the olivines have been totally altered) varies widely. Site 250 contains an aluminian, titaniferous salite and An_{74}; Site 251, augite and An_{65}; Site 254, augite and An_{68}; Site 256, augite and An_{55-60}; and Site 257, endiopside phenocrysts and augite groundmass, with zoned plagioclase phenocrysts (An_{63-91}, typically An_{87}) and groundmass An_{73}. The phenocrysts in Site 257 are regarded as highly basic or "primitive", while the range in plagioclase compositions at Sites 256 and 257 is remarkable.

Chemically, the main features are the relatively high potash and rubidium of the Site 250 basalt; the picritic nature (rich in magnesia [14%], chromium, and nickel) of one Site 253 basalt; and the striking depletion in magnesium, chromium, and nickel, and enrichment in iron, vanadium, and titanium of the very homogeneous olivine-poor, highly fractionated Site 256 basalts. By comparison, the "primitive" Site 257 basalts show none of these features. Division into high- and low-alumina, olivine, or plagioclase, or high-alumina plagioclase, plagioclase, and pyroxene tholeiites is generally unsuccessful.

Normatively, basalts from Sites 251, 253 flow, 256, and 257 are quartz tholeiites; possibly the basalt from Site 254 belongs in this category also. Alteration, involving oxidation of ferrous iron to ferric, increases quartz-normativeness (as does the presence of calcite) but normalization on a calcite-free, $Fe_2O_3 = 1.5\%$ basis confirms the quartz-normative character of the rocks. Possibly, loss of silica through alteration can override oxidation of the iron (?as at Site 254) to produce highly olivine-normative rocks. Thus, the quartz-normative nature of many of the Leg 26 basalts is believed to be a real characteristic which may apply to many drilled (and, therefore, structurally deep) basalts, as opposed to dredged (from ridge flanks and slopes) basalts, which are commonly olivine tholeiites.

Differentiation at Sites 256 and 257, through crystallization fractionation, has resulted in strikingly different trends. Plotted against depth, Site 256 shows slight normal iron-enrichment but abnormal lime-enrichment up the hole. Site 257, on the other hand, with eight

---

[1]Analyses by V. K. Din, C. J. Elliott, J. C. Leverton and R. F. Symes, Department of Mineralogy, British Museum (Natural History), London, England and additional notes on Uranium distribution by J. D. Kleeman, Department of Geology, University of New England, Armidale, N. S. W. 2351, Australia.

or more flows measuring 64.5 meters in total thickness, shows normal alkali-enrichment but abnormal iron-depletion up the hole. Partial melting of an already differentiated magma, or differentiation of slowly rising magma, could explain the abnormal fractionation trends.

INTRODUCTION

The amount of igneous/metamorphic rock recovered on Leg 16 (68.6 m) is second only to that from Leg 24 (74 m). (Of the total DSDP hard-rock recovery [31 legs], 46% was taken from the Indian Ocean [Vallier, personal communication; Freisen, 1973]).

Basalt was cored at six of the nine sites on Leg 26 (Figure 1). Basement was not reached at Sites 252, 255, or 258. In each case the basalt appears to form the basement, although in the case of Site 253 it may have been intruded into the sediments as a sill. The fresh basalts from Sites 251, 256, and 257 (Figure 1) are low-K_2O, ocean-floor tholeiites, containing normative quartz. Chemically, basalt from Site 250 appears to have calc-alkaline affinities while the two Ninetyeast Ridge sites (253 and 254) yielded highly altered olivine-normative rocks and one quartz-normative rock. The origin of the latter rocks is discussed elsewhere (Frey et al., this volume, Chapter 23) but an account of their petrology is included here. The possible basement rock at Site 253 is a picritic basalt, overlain by 400 meters of ash, also described elsewhere (McKelvey and Fleet, this volume, Chapter 22), containing two thin, glassy scoriaceous basalt flows.

Many of the basalts at Site 257, where a total of 64.5 meters of igneous rock was drilled, are extremely fresh. This thick sequence, approaching the record-to-date (through Leg 31) of 80 meters at Site 238, Leg 24, has a high acoustical velocity, increasing almost linearly with depth (Hyndman, this volume, Chapter 16). In this and other respects, the two series of basalts, emplaced as multiple flows, are very similar (Bunce and Fisher, in preparation); possibly a series from Site 251, were it available, would show similar features (Figure 1).

Age determinations (K-Ar) were carried out on a total of eight samples, of which the last three, two whole rocks and one feldspar phenocryst concentrate, are from Site 257. The ages are shown in Table 1 and a full discussion is given elsewhere (this volume, Chapters 17 and 36). It should be noted that the samples were found to be unusually rich in hydrocarbons, especially methane. The flows at Site 257 show a K-Ar age spread of 100 m.y. They include several red-chalk layers and also contain a 60-cm clay band, possibly a "laterite" resulting from a diastem or erosion interval, proving that the basalts were deposited as flows, not intruded as sills. This fact is significant in the light of the unusual fractionation features shown by the basalts at this site, discussed in a later section.

There is a remarkable textural variation in the basalts, which range from glassy through variolitic and hyalophitic to fairly coarse subophitic or diabasic. Only the basalts at Sites 253 and 257 are truly porphyritic. They are also highly vesicular, and alternately subophitic and subvariolitic (feathery). The vesicularity suggests eruption in shallow water or even subaerially. Pillow structures were noted only at Site 251, but at Site 238 (Leg 24), on the Central Indian Ridge, pillows with glassy selvages have been reported (Bunce and Fisher, in preparation). None of the basalts recovered is chemically spilitic. At Sites 250, 256, and 257 the rocks are extensively veined by, or have vesicles filled with, celadonite. This glauconitic mineral, with a spectacular, vivid green color, is unusually common; it is described in a later section.

TABLE 1
Whole Rock K-Ar Age Determinations on Basalts from Leg 26[a]

Sample	Depth Below Sediment/Basalt Contact (m)	Age (m.y.)	Degree of Error (±)	Reliability Grades[b] *	†
250-26-6	17.0	89	6.0	B	B
251-31-4	8.0	39	2.0	D	A
253-58-1	0.0	101	3.0	C	D
254-35-1	18.0	49	5.0	B	D
256-10-2	8.0	92	4.0	A	C
257-11-2	3.5	92	7.0	B	B
257-13-3	24.0	174	10.0	–	–
257-16-2[c]	48.0	157	5.0	C	A
257-17-5	61.5	196	9.0	B	A

[a]Analysts: N.J. Snelling and C. Rundle, Institute of Geological Sciences, London.
[b]Subjective estimates, taking into account contamination by atmospheric argon (*), and alteration (†). A, high; D, low.
[c]Carried out on a plagioclase feldspar phenocryst concentrate (K_2O, 0.03%). This age may not be as reliable as those above and below it.

PETROGRAPHY

The petrography of the basalts is summarized in Tables 2 and 3.

Site 250

At the first site, in the Mozambique Basin (Figure 1), a thickness of 18 meters of basalt was drilled. The rock shows moderate alteration for the upper 14 meters, the uppermost 4 meters being traversed by numerous calcite and serpentine-filled veins and fractures. Near the contact with the sediments, which is apparently normal and conformable, with no baking of the overlying clay (which fills cavities in the uppermost basalt), the rock is sparsely vesicular. The vesicles are filled with calcite or with vivid green celadonite (described in a later section), which also veins the rock.

The uppermost rock is reddish-brown and subvariolitic in texture (Plate 1, Figure 1), similar to the rock from *Mahabiss* Station 133 (Plate 1, Figure 2), on the equatorial Central Indian Ridge. Below, the basalt is dark gray, while the texture coarsens and becomes subophitic (Plate 1, Figures 3, 4). This rock is fairly fresh. Probably, several flows are present.

The bulk of the rocks comprises pyroxene and plagioclase (An_{74}), with olivine altered to iddingsite-bowlingite and skeletal iron ore, probably ilmenite. The coarser

TABLE 2
Visually Estimated Typical Modes of Non-Glassy Basement Basalts

Site	Olivine (Fresh or Altered)	Pyroxene	Plagioclase	Iron Ore	Accessories (Apatite, Quartz, etc.)	Glass or Mesostasis	Thickness of Basalt Drilled (m)
250	12	37	31	8	–	12	18.00
251	T	38	43	9	T[a]	10	12.50
253	15	–	20	6	T	59	0.35
254	1	31	35	3	–	30	42.50
256	1	32	35	10	–	22	19.00
257	3	37	38	7	–	15	64.50

[a]T = trace

TABLE 3
Summary of Characteristics of Some Analyzed Basaltic Rocks

Sample	Condition	Texture	Co-ordinates in Triple Triangular Diagram[a]	Olivine (Altered)	Maximum Length (mm)	Pyroxene Composition (av.)	Maximum Length (mm)	Plagioclase Composition (av.)	Maximum Length (mm)
250A-26-6, 45-47 cm	Fresh	Subophitic	$di_{39.1}{}^{hy}{}_{31.2}{}^{ol}{}_{29.7}$	Common	0.6	$Mg_{41}Fe_{11}Ca_{48}$	1.2	An_{74}	0.9
251A-31-4, 29-31 cm	Fresh	Coarse, subophitic	$qz_{2.7}{}^{di}{}_{47.4}{}^{hy}{}_{49.9}$	Rare	0.3	$Mg_{44}Fe_{18}Ca_{38}$	1.0	An_{65}	2.5
253-24-1, 84-85 cm	Fairly altered	Scoriaceous, glassy	$qz_{14.6}{}^{hy}{}_{85.4}$	Common (fresh in glass)	0.6 2.0	n. d.	–	n. d.	0.8
253-58-1, 2-7 cm	Altered	Glassy to subvariolitic, porphyritic	$di_{1.5}{}^{hy}{}_{56.9}{}^{ol}{}_{41.6}$	Very common	1.0	n. d.	–	n. d.	0.2 to 1.8
254-36-3, 95-97 cm	Highly altered	Hyalo-ophitic	$qz_{6.0}{}^{di}{}_{27.8}{}^{hy}{}_{66.2}$	Rare	0.5	$Mg_{40}Fe_{18}Ca_{42}$	1.2	An_{68}	1.8
254-38-1, 115-117 cm	Highly altered	"Non-igneous"	$qz_{10.4}{}^{di}{}_{15.9}{}^{hy}{}_{73.7}$			n. d.	–	n. d.	–
256-9-3, 45-47 cm	Fairly altered	Hyalo-ophitic	$qz_{7.1}{}^{di}{}_{49.7}{}^{hy}{}_{43.2}$	Scarce	0.5	n. d.	1.5 (Clusters)	n. d.	1.3
256-10-2, 87-90 cm	Fairly altered	Subophitic	$qz_{12.0}{}^{di}{}_{38.5}{}^{hy}{}_{49.5}$	Very rare		$Mg_{48}Fe_{17}Ca_{35}$	0.5	$An_{55\text{-}60}$	0.9
256-11-3, 110-113 cm	Fairly altered	Subophitic	$qz_{10.4}{}^{di}{}_{42.3}{}^{hy}{}_{47.3}$			n. d.	0.5	n. d.	1.5
257-11-2, 82-84 cm	Fresh	Hyalo-ophitic	$qz_{4.0}{}^{di}{}_{46.2}{}^{hy}{}_{49.8}$			$Mg_{50}Fe_{8}Ca_{42}$	1.0	An_{72}	1.0
257-14-4, 124-126 cm	Fresh	Subophitic, porphyritic	$qz_{6.2}{}^{di}{}_{45.5}{}^{hy}{}_{48.4}$	Rare	0.8	$Mg_{52}Fe_{8}Ca_{40}$	1.5	An_{90}	4.0 (Phenocrysts)
						$Mg_{50}Fe_{12}Ca_{38}$	0.5	An_{74}	0.8 (Groundmass)
257-15-1B, 126-128 cm	Fresh	Subophitic, porphyritic	$qz_{5.7}{}^{di}{}_{48.6}{}^{hy}{}_{45.7}$			$Mg_{52}Fe_{10}Ca_{38}$	0.7	An_{86}	2.5
257-16-2, 94-96 cm	Fresh	Subophitic, porphyritic	$qz_{4.9}{}^{di}{}_{51.8}{}^{hy}{}_{43.3}$			$Mg_{46}Fe_{12}Ca_{42}$	–	$An_{91\text{-}63}$	4.5 (Phenocrysts)
						$Mg_{47}Fe_{22}Ca_{31}$	1.5	An_{75}	0.8 (Groundmass)
257-17-5, 65-67 cm	Fresh	Hyalo-ophitic	$qz_{3.9}{}^{di}{}_{50.6}{}^{hy}{}_{45.4}$	Rare	0.5	$Mg_{50}Fe_{10}Ca_{40}$	0.7	An_{76}	1.2

Note: n.d. = not determined.
[a]From Tables 5, 6.

subophitic basalt is notable in containing abundant clove-brown "titanaugite" ($Mg_{41}Fe_{11}Ca_{48}$). Although the olivine is invariably altered, the rocks from this site and from the two Ninetyeast Ridge sites are normatively and modally the most olivine-rich of all those analyzed from Leg 26. The remainder of the basalts, and the bulk of the glassy, variolitic types, consists of a dark reddish-brown, more- or less-devitrified mesostasis, probably largely a smectite.

Site 251

The basalt at this site on the flank of the Southwest Branch appears to be a pillow lava, with which the overlying garnet-bearing calcite (micarb) chalk (Kempe and Easton, this volume, Chapter 25) forms a normal contact. Three loose cobbles were recovered from Core 29, comprising tachylyte or reddish-brown glassy basalt. The glassy basalt is rimmed by mantles of pale basalt glass ($n = 1.602$, typical of sideromelane). The glass, and, to a much greater extent, the glassy basalt, have devitrified, and contain circular variolites of radially arranged microlites, small olivine crystals, and minute flow-aligned acicular olivines and plagioclase laths (Plate 1, Figure 5). The thin section of this rock contains one large (6 mm) glomerophyric cluster of labradorite crystals.

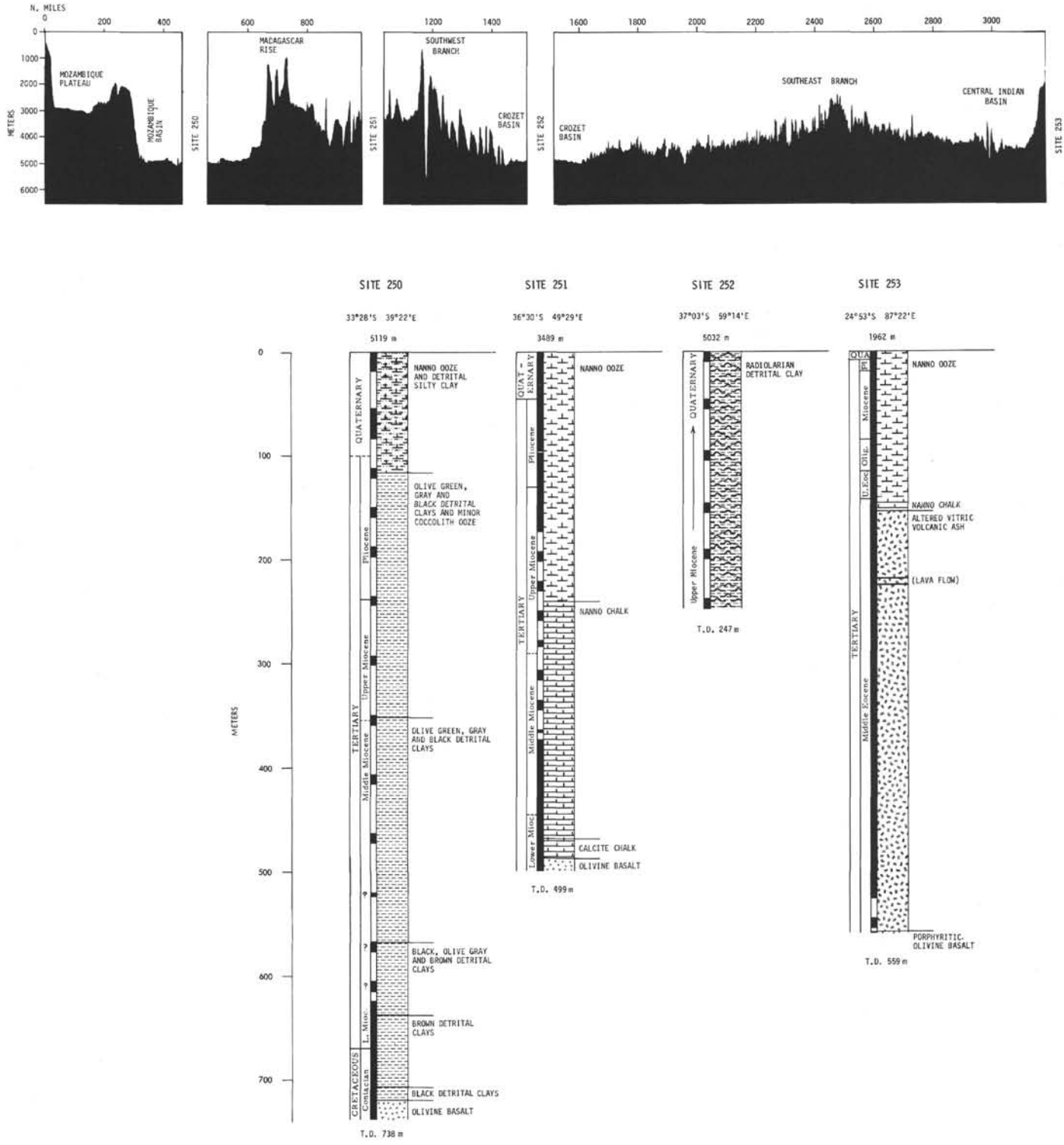

Figure 1. *Schematic summary profile across the Indian Ocean (DSDP Leg 26).*

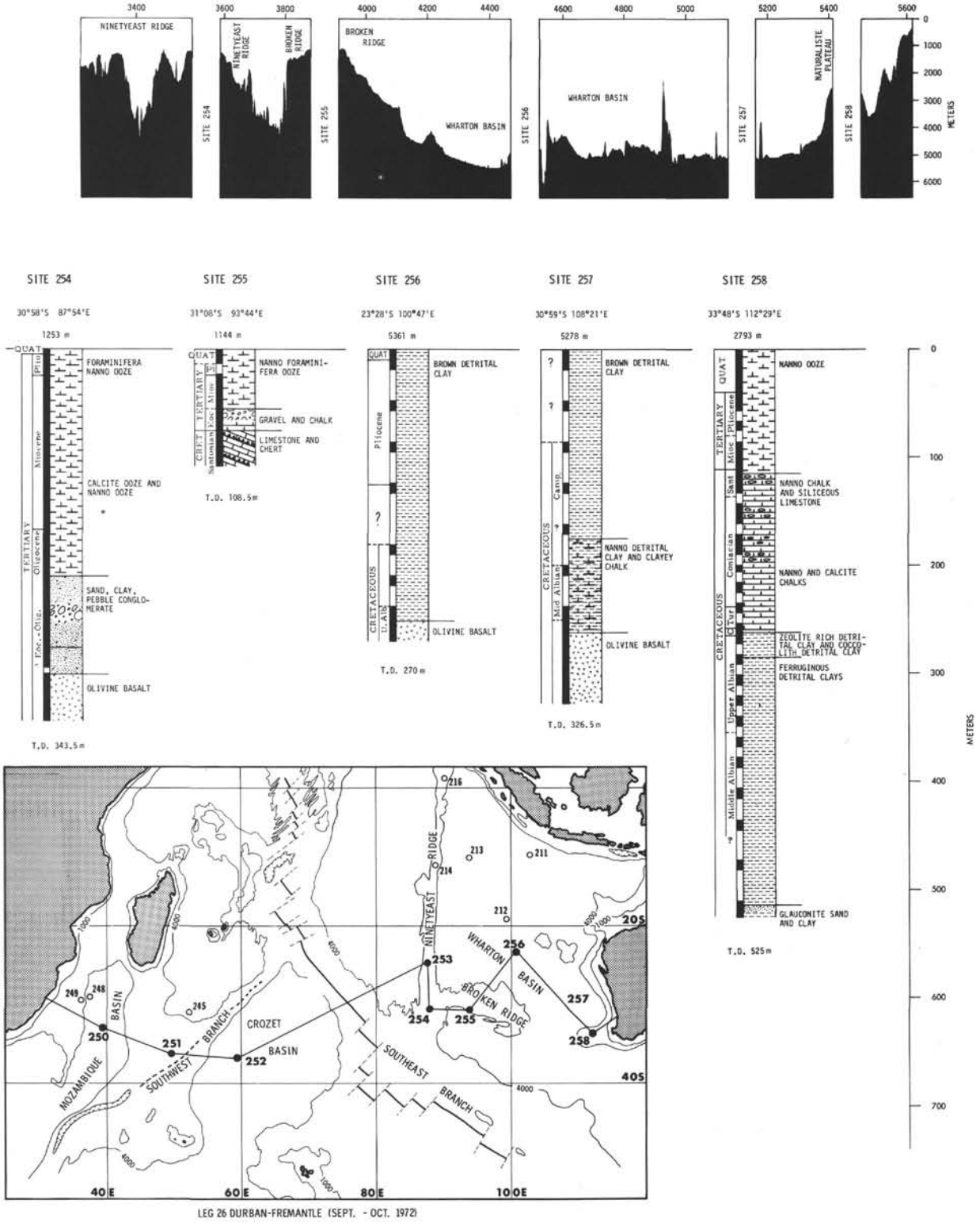

LEG 26 DURBAN-FREMANTLE (SEPT. - OCT. 1972)

Figure 1. *(Continued).*

Core 31 consists of veined, altered, highly vesicular basalt developing rapidly downwards into coarse subophitic basalt, and as at Site 250, is fairly fresh. This rock has the coarsest texture of any drilled on Leg 26 (Plate 1, Figure 6). It consists largely (Table 2) of zoned plagioclase laths (An_{65}), pyroxene ($Mg_{44}Fe_{18}Ca_{38}$), and granular iron ore. At the higher levels a few totally altered olivine crystals are present and the interstitial mesostasis is glassy. Below, olivine is absent and there is a well-crystallized mesostasis, containing smectite, feldspar, iron oxide, and, locally, quartz. One aspect of the subophitic texture in the very coarse rocks is remarkable: the plagioclase laths are deeply embayed (Plate 2, Figure 1) and indicate that they have formed around the pre-existing nodular or granular pyroxene. This texture has been noted in coarse ophitic basalts (or dolerites) dredged off Dronning Maud Land, Antarctica (Kempe, 1973b).

Site 253

The thick (400 m) Eocene ash sequence at this Ninetyeast Ridge site is described in detail by McKelvey and Fleet (this volume, Chapter 22). The origin of the basalts from this site and of the Ridge itself, taking into account the results obtained on Leg 22, is discussed by Frey at al. (this volume, Chapter 23).

In summary, the sequence comprises a sequence of hyaloclastic and pyroclastic rocks (vitric ash and lapilli) within which are two thin scoriaceous olivine basalt flows and below which, apparently as basement, lies altered olivine-rich glassy picritic basalt.

The upper flow consists of dark, reddish-brown partly palagonitized glass bordering scoriaceous glassy olivine basalt. Fresh olivine crystals are common in the glassy section, along with small laths, prisms, and rhombs of plagioclase (Plate 2, Figure 2). Where fresh, the glass (Plate 2, Figure 3) is a clear, almost colorless sideromelane, very similar to that dredged from Expedition DODO Station 113 (Engel, Fisher, and Engel, 1965) (Plate 2, Figure 4). Palagonitization has taken place locally in round and irregular spherulitic patches, sometimes filled with radially arranged, fibrous prisms (length slow) of phillipsite. This zeolite has the large cell dimensions associated with authigenic growth in deep-sea sediments, as found, for example, at DODO Station 113 (Sheppard et al., 1970), rather than the smaller structure found in phillipsite taken from cavities in continental basalts. The remainder of the flow consists of scoriaceous palagonite containing altered olivines and plagioclase laths.

The glassy to subvariolitic porphyritic olivine basalt in which the hole was terminated is the richest in olivine (normatively and modally) of any basalt drilled on Leg 26 (~15%). The rock is highly altered, the euhedral olivine crystals being replaced by serpentine and talc. Plagioclase laths and skeletal and granular iron ore make up the other crystalline phases, accompanied by a few tiny, sharply euhedral dipyramidal anatase crystals. Pyroxene is not visible but is probably present, with the other mineral phases and glass, in the fine-grained matrix of the rock (Plate 2, Figures 5, 6).

Site 254

The second Ninetyeast Ridge site is also discussed by Frey et al. (this volume, Chapter 23). The lowest sedimentary unit is a clay-sand-conglomerate sequence, iron-enriched at the base, and apparently largely derived from the weathering of basalt, possibly in situ since there are no proven pyroclastics. This sequence contains a 2-meter flow of basalt about 25 meters above the basement. The contact with the basment is apparently normal.

Three types of basalt were recovered from this hole, in what appears to be the reverse of the order that might be expected from their chemistry and degree of alteration. These rocks form the second longest section of basalt drilled on Leg 26 and are by far the most altered. Several flows must be present. Of the three basalt types the highest, including the intersedimentary flow, consists of fairly coarse hyalo-ophitic basalt (Plate 3, Figure 1), containing quite large (3 mm) feldspars. In these, ophitic clusters of pyroxene ($Mg_{40}Fe_{18}Ca_{42}$) and feldspar (An_{68}) are set in a palagonitic glassy matrix. A few completely altered olivine crystals are present, with ilmenite and pools of calcite. Below the ophitic basalt are amygdaloidal lavas, the amygdales filled with green spherulitic bowlingite (or chlorite), or calcite; some have both, in which case the calcite always occupies the center (Plate 3, Figure 2). Fairly abundant olivine is present in these rocks and is altered to iddingsite, showing the characteristic pleochroism, birefringence, and lamellar structure. This group includes some non-amygdaloidal lavas (Plate 3, Figure 3) which are otherwise similar. Finally, there is a group of unusual, completely altered, possibly autobrecciated, basalts (Plate 3, Figure 4). In some, the original basaltic texture has very largely been destroyed and replaced by a vesiculated texture in which the minerals are shown by X-ray diffraction to consist of 60-70% smectite accompanied by more or less equal quantities of feldspar, amphibole, pyroxene, and quartz. Possibly, some of the rocks once contained appreciable amounts of olivine but it cannot be stated with certainty on the evidence of the shapeless secondary minerals. Plagioclase, pyroxene, and ilmenite are recognizable and the rocks grade into varieties that are considerably less altered. The autobrecciated group contains abundant xenoliths of basalt and the drilling log records considerable variations in hardness within the amygdaloidal and brecciated rocks.

Site 256

Basement was reached at both of the Wharton Basin sites. At the first (Site 256), a sequence of graded flows (at least four) was drilled, each flow grading downwards from fine- to coarser-grained basalt. The rocks are not very fresh and contain the least olivine of those drilled on Leg 26. In texture, they vary from glassy and subvariolitic (Plate 4, Figure 1) to hyalo-ophitic and subophitic (Plate 3, Figure 5, 6; and Plate 4, Figure 2). The mineralogy is simple: laths and squarish prisms of plagioclase (An_{55-60}) and clusters of pyroxene ($Mg_{48}Fe_{17}Ca_{35}$) crystals, with ilmenite and glass. The

texture is locally glomeroporphyritic but does not achieve the strongly porphyritic character of the second Wharton Basin basalt (Site 257). Olivine is sparsely present, especially in the middle grain-size range, and always totally altered. Near the upper contact with the overlying clay, slight brecciation has taken place, incorporating fragments of finer-grained basalt. Also, at the contact, veining and fracturing has occurred, the vein materials being calcite, often spherulitic, and vivid green celadonite. This "glauconitic" mineral also penetrates the texture of the basalt here, apparently replacing prisms of pyroxene.

Site 257

A similar sequence of at least seven or eight graded flows was drilled at the second Wharton Basin site. The total thickness of 64.5 meters is the deepest penetration into basalt on the Leg and the basalt is the freshest. The contact with the overlying red clay is normal and the sequence contains a 60-cm-thick interbasaltic sedimentary interval in Core 15. Most of the other cores have a brown and red recrystallized fossiliferous limestone interval at the top, up to 10-cm thick, baked by the overlying flow.

The basalt sequence alternates between fine- and medium-grained rocks, there being several very thin flows (?or pillow layers) so that the total number drilled may well exceed eight. The rocks are highly vesicular, suggesting eruption in shallow water, and the vesicles are frequently filled with celadonite, which also occurs, with calcite, in veins. The sequence is highly fractured, especially in the upper, altered parts, where the filling and surface filming material is usually serpentine or chlorite. There are brecciated areas, possibly resulting from contact of the hot lava with cold seawater, recemented with calcite; like the basal sediment, the carbonate is red due to iron staining. The calcite occurs as spherulitic, botryoidal encrustations and is occasionally found in vugs in well-formed scalenohedral crystals.

The upper, finer-grained parts of each flow consist of highly vesicular glassy or subvariolitic basalt (Plate 4, Figures 5, 6; and Plate 5, Figures 1, 6); the lower and more abundant are coarser porphyritic, hyalo-ophitic or subophitic rocks (Plate 4, Figures 3, 4; and Plate 5, Figures 2-5). The sequence becomes generally less vesicular and more porphyritic downward, although the deepest core is almost completely aphyric. As already stated, this sequence contains most of the only truly porphyritic basalts recovered on Leg 26.

In the coarser porphyritic rocks, zoned plagioclase (phenocrysts, An_{63-91}; groundmass, An_{74}) and pyroxenes (phenocrysts, $Mg_{49}Fe_{10}Ca_{41}$; groundmass, $Mg_{50}Fe_{13}Ca_{37}$) are again the main constituents, the larger phenocrysts of feldspar reaching 4.5 mm and of pyroxene, 1.5 mm. The groundmass pyroxene forms radial fan-like bunches. Olivine is more abundant than at Site 256, always totally altered (sometimes to smectite), while skeletal ilmenite and an interstitial mesostasis of palagonite complete the rock. The fine-grained, glassy rocks contain less olivine, with plagioclase and pyroxene in grains or spherulitic rosettes, in a feathery devitrifying and subvariolitic groundmass. The many vesicles are filled with calcite, palagonite, or vivid green celadonite. The fine subophitic, semiporphyritic basalt of Sample 257-15-2, 37 cm (Plate 5, Figure 4) has embayed plagioclase laths, formed around pre-existing pyroxene, as are found in the coarse subophitic basalt at Site 251 (Plate 2, Figure 1).

CELADONITE

The vivid green mineral veining the basalt at Sites 250, 256, and 257, filling vesicles with smectite at Site 257, and "replacing" laths of plagioclase or pyroxene at Site 256, has been identified by X-ray powder photography as glauconite. Subsequent chemical analysis confirmed it as the magnesium-rich, aluminum-poor variety, celadonite. This mica usually occurs in the uppermost, most altered part of the basalt sequence (though it extends downwards a considerable distance in Site 257), is nearly always associated with calcite and, probably coincidentally, was found only in the deep basin sites, not in the three ridge basalts.

The three different habits have distinct characteristics. In veins, celadonite occurs as a "spiky" growth of apple-green radial fibers into calcite (Figures 2, 3). At magnifications of about $\times 5000$, the vein celadonite can be seen to consist of an aggregate of minute plates (Figure 4), as stated by Hendricks and Ross (1941, p. 685). In vesicles, the vivid green celadonite forms close-packed radially arranged fibers, while in localized areas of two rocks it apparently replaces plagioclase, pyroxene, and, possibly, olivine. This is the opposite to the normal replacement of olivine and, sometimes, hypersthene (Hendricks and Ross, 1941, p. 685). These habits can be seen in Plate 3, Figure 5 and Plate 4, Figure 6. The mineral is strongly pleochroic from pale apple-green to darkish blue, the pleochroism being most marked in the prismatic replacement habit, with blue (maximum absorption) lying parallel to the long direction of the "prisms". The celadonite is birefringent and usually extinguishes parallel to the prismatic outlines.

A chemical analysis of the vein celadonite, together with its structural formula on the basis of 24(O,OH,F), is given in Table 4, determined by atomic-absorption and microprobe methods, for which, apart from the K_2O content, agreement is good. For comparison, the nearest analysis from the range of continental basalt occurrences given by Hendricks and Ross (1941, p. 697), from Madagascar, is also shown. Ferri-celadonite has been reported from Leg 15 basalts from the Caribbean (Bence et al., 1973b) and from Leg 17 basalts from the Central Pacific Basin (M. N. Bass, personal communication). It is interesting that celadonite, rather than glauconite, occurs in oceanic basalts, following its chemical affinity with these rocks. Glauconite, although a common marine mineral, does not appear to be known from basalt. In this way, celadonite is the reverse of phillipsite, the deep-sea sedimentary variety of which occurs at Site 253, filling vesicles in basalt; it does not occur in its continental form which is only known from vesicles in terrestial basalts.

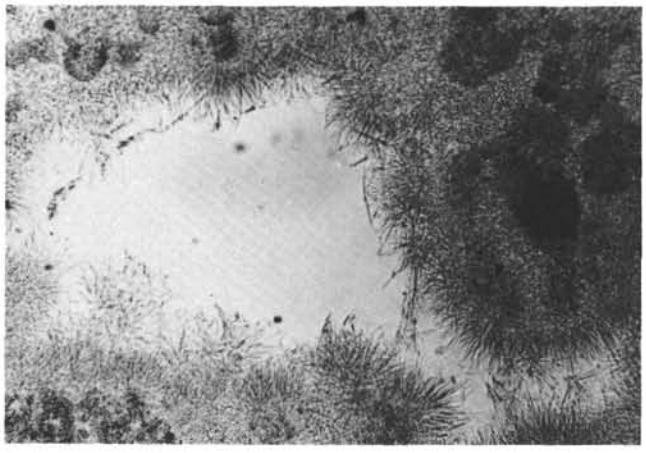

Figure 2. *Photomicrograph of celadonite vein in basalt. (Sample 250A-25-1, 110 cm). Plane polarized light, X 206.*

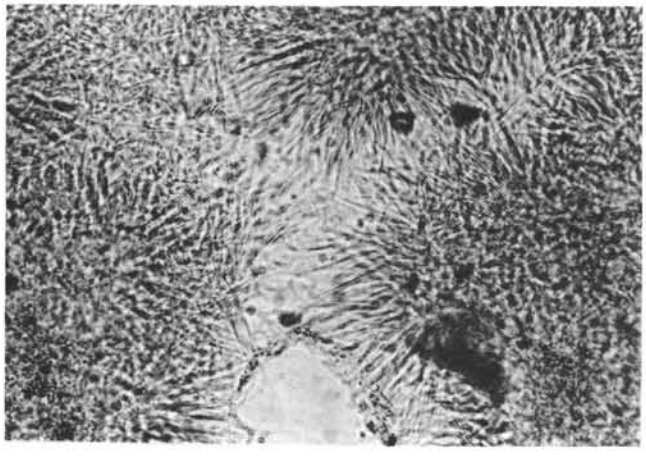

Figure 3. *Photomicrograph of celadonite vein in basalt. (Sample 250A-25-1, 110 cm). Plane polarized light, X 476.*

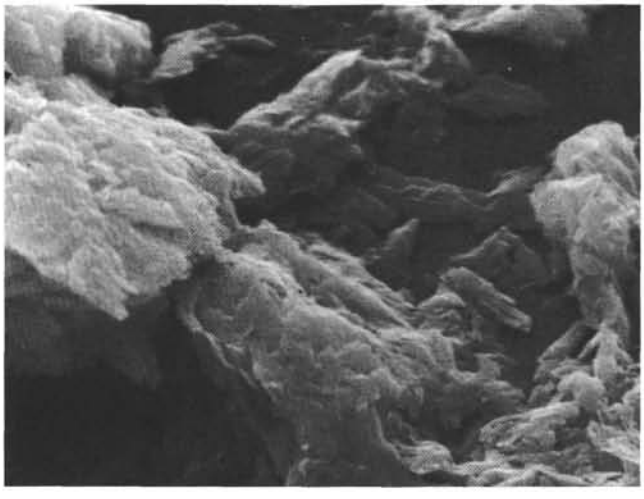

Figure 4. *SEM photograph by H.A. Buckley (gold coating) of celadonite in vein in basalt. (Sample 250A-25-1, 110 cm). X 3500.*

CHEMISTRY

Twenty-three of the basalts were analyzed and some of their trace elements determined (Tables 5, 6). From Sites 256 and 257 a series of three and twelve analyses, respectively, were made to determine if any vertical differentiation or other variation were apparent. From Sites 250 and 251, one analysis typical of the fresh basalts from each was made, with two analyses of the altered rocks from Site 251. Finally, from each of the two Ninetyeast Ridge sites (Sites 253 and 254) two analyses were made; from Site 253, analyses of a scoriaceous flow and of the "basement"; and from Site 254, analyses of the basement and of one highly altered rock to see if its chemistry suggested spilitization. Some comparative average compositions are shown in Table 7.

Of the 23 basalts selected, omitting the three deliberately selected for their altered states, those from Sites 250, 251, and five from Site 257 are fresh, using the criteria of Miyashiro et al. (1969) that Fe_2O_3 should not exceed 2.0%, nor the Fe_2O_3/FeO ratio 0.3. Those from Sites 253 and 256 are not fresh while those from Site 254, especially the second analysis, show a high degree of alteration. Although the low content of CaO (6.6%) suggests possible initial spilitization (Cann, 1969), the low Na_2O (1.9%)shows that this rock is not a spilite. No other analysis suggests spilitization, but the extremely low Na_2O content in the Site 253 "basement" basalt (1.4%) is remarkable. This talc (olivine)-rich rock has a very high MgO (and low MnO) content (14%), suggesting a picritic (oceanitic) composition. With a value of 21.7% for (CaO + MgO), this rock lies outside the compositional limits of 12 to 20% (CaO + MgO) chosen by Pearce and Cann (1973) to define their selection of essentially basaltic rocks. So, however, do 9 of the 12 analyzed Site 257 basalts, with an average value of 20.3%. The water content is variable; high H_2O^+ values for Site 253 (basement) and Site 254 (altered rock) are notable, while H_2O generally follows high Fe_2O_3 to indicate lesser alteration, although the level at Site 256 is not appreciably higher than at Site 257. There appears to be very little correlation between degree of alteration (with consequent increase in K_2O, resulting in too low an age) and reliability of the age determinations given in Table 1 (Hart and Nalwalk, 1970; Dymond, 1973). Deep-drilled basalts should provide ideal material for testing the hypothetical reactions between basalt and sea water proposed by Hart (1970) and Melson (1973) involving often considerable gains of potassium, titanium, and total iron, as well as water, and losses of calcium, magnesium, and silicon, accompanied by oxidation of ferrous iron to the ferric state. Movement of aluminum, sodium, manganese, and phosphorus is less clearly defined.

The basalt analyses span a considerable range in silica content, from 43.4 to 50.5%, while the K_2O content is generally low, indicative of oceanic tholeiites (Engel, Engel, and Havens, 1965). Two of the analyses of the deepest of the basalts from Site 257, with K_2O of 0.04%, are among the lowest on record for this oxide, especially among published Indian Ocean basalt analyses. The analysis of the Site 250 basalt, with K_2O of 0.6%, suggests that it has calc-alkaline affinities. Subdivision on the basis of composition along the lines suggested by

TABLE 4
Chemical Analysis of Celadonite

	Sample 250A-25-1, 135 cm		
	Atomic Absorption[a]	Electron Microprobe[b]	Continental Basalt Occurrence[c]
SiO_2	54.97	55.80	54.30
TiO_2	0.26	0.29	–
Al_2O_3	5.02	5.76	5.08
Fe_2O_3	12.87	12.25	14.77
FeO	3.56	3.42	4.82
MnO	0.07	–	0.09
MgO	6.77	6.78	6.05
CaO	0.15	0.36	0.80
Na_2O	0.67	0.81	3.82
K_2O	7.43	9.28	4.85
H_2O+	5.64	5.64	5.64
H_2O-	3.23	3.23	–
Totals	100.64	103.62	100.22
	Numbers of ions on the basis of 24 (O, OH, F)		
Si	7.705	7.656	7.76
Al	0.295	0.344	0.24
	8.00		8.00
Al	0.534	0.588	0.60
Ti	0.027	0.030	–
Fe^{3+}	1.358	1.265	1.60
Fe^{2+}	0.417	0.392	0.58
Mn	0.008	–	–
Mg	1.414	1.386	1.28
	3.76		3.66
Ca	0.023	0.053	
Na	0.182	0.215	
K	1.329	1.625	
	1.53		1.89
F	–	–	–
OH	5.274	5.162	–
	5.27		5.16
			4.06
			1.92

[a]Analyst: C.J. Elliott
[b]Analyst: J.C. Leverton
[c]Celadonite, Madagascar (Lacroix, 1916). Analyst: M. Raoult

Miyashiro et al. (1969) for the grouping of tholeiites from the Mid-Atlantic Ridge into low- and high-alumina tholeiites, showing variation in MgO and FeO*/MgO ratio (where FeO* represents total iron as FeO) owing to crystallization differentiation, has a limited application, since the analyzed basalts derive from a wide variety of environments. It can be applied to the 3 analyses from Site 256 and the 12 analyses from Site 257. The analyses from Site 256 show a remarkable degree of homogeneity and are very highly fractionated (iron-enriched), with slight differentiation within the three. At Site 257 there is far greater compositional variation and, with some exceptions, a near-linear crystallization-differentiation trend with depth can be demonstrated. Yeats et al. (1973), discussing the chemistry of basalts from the eastern Pacific Ocean (Leg 16), demonstrated that a series of rocks shows decreases in TiO_2 and Na_2O, and an increase in CaO, with distance from the crest of the East Pacific Rise. Such changes could only be expected on Leg 26 between basalts from the Sites 250 and 251, and possibly Sites 256 and 257 (Figure 1). In the case of the former, no such changes are apparent; in the case of the latter, there are marked decreases in TiO_2 and Na_2O, and an increase in CaO, between the analyses of basalts from Sites 256 and 257. There appear, however, to be fundamental differences between the basalts from those two sites, noted below.

There is, thus, no clear division of the Leg 26 basalts into low- and high-alumina tholeiites, using the values of Miyashiro et al. (1969). The Al_2O_3 content of the Leg 26 basalts lies between 13 and 17.4%. It is becoming apparent, however, that drilled basalts seem to be appreciably poorer in Al_2O_3 than dredged samples (Shido et al., 1971), often with a content well under 15%. The

TABLE 5
Chemical Analyses of the Basalts from Sites 250, 251, 253, 254, and 256[a]

	Sample										
	250A-26-6, 45-47 cm	251A-30-1, 140-145 cm	251A-31-1, 39-41 cm	251A-31-4, 29-31 cm	253-24-1, 84-85 cm	253-58-1, 2-7 cm	254-36-3, 95-97 cm	254-38-1, 115-117 cm	256-9-3, 45-47 cm	256-10-2, 87-90 cm	256-11-3, 110-113 cm
SiO_2	47.72	45.89	45.68	50.37	49.48	43.42	44.59	45.26	49.59	48.76	49.26
TiO_2	1.46	1.47	1.78	1.60	0.93	0.69	2.47	1.58	2.50	2.55	2.48
Al_2O_3	16.33	13.44	15.65	14.60	17.39	15.61	13.93	13.19	13.31	12.93	13.30
Fe_2O_3	1.70	6.77	8.05	1.70	2.54	3.23	5.59	7.20	3.06	3.55	3.58
FeO	6.43	5.14	5.31	8.74	4.28	6.87	7.62	5.04	10.21	9.83	9.56
MnO	0.14	0.18	0.18	0.17	0.05	0.11	0.18	0.12	0.23	0.17	0.18
MgO	8.76	7.43	4.88	7.13	7.46	13.85	7.65	10.18	6.06	6.02	6.22
CaO	10.86	11.48	10.96	10.84	9.17	7.84	9.39	6.62	10.43	9.71	9.62
Na_2O	2.72	2.57	2.58	2.67	2.89	1.39	2.48	1.94	2.66	2.67	2.68
K_2O	0.57	0.30	0.60	0.12	0.30	0.37	0.15	0.68	0.24	0.24	0.25
H_2O^+	2.26	1.47	1.16	0.90	0.80	4.42	1.72	4.09	0.60	0.90	0.65
H_2O^-	0.78	2.17	1.95	0.62	3.52	2.71	2.53	3.89	1.05	1.37	1.43
P_2O_5	0.25	0.16	0.27	0.15	0.33	0.08	0.26	0.17	0.25	0.22	0.26
CO_2	0.88	1.60	1.53	0.23	1.62	0.38	1.21	0.27	0.28	0.97	0.39
Others	0.15	0.01	0.02	0.16	0.04	0.15	0.23	0.04	0.19	0.18	0.18
Total	101.01	100.08	100.60	100.00	100.80	101.12	100.00	100.27	100.66	100.07	100.04
Trace elements (ppm)											
Ti	8753	8812	10,671	9592	5575	4137	14,808	9472	14,988	15,287	14,868
Ga	50			50		25	50		50	50	40
Cr	215	245	245	220		325	280		105	110	110
Li	15	55	55	12		18	⩽ 5		7	8	7
Nb	<50			<50	<50	<50	<50	<50	<50	<50	<50
Ni	110	170	165	110		310	200		130	110	100
Cu	12	70	70	12		12	115		17	12	12
V	250	285	285	370		250	400		450	490	470
Zn	70	100	105	115		50	125		130	125	125
Zr	200			200	200	50	200	200	200	200	200
Y	25			50	50	25	50	50	50	50	50
Sr	210	85	85	80		50	155		165	160	160
Pb	–			–		–	–		–	–	–
Ba	110	130	200	25		10	85		25	40	25
Rb	< 5	6	9	< 5		< 5	< 5		< 5	< 5	< 5
Norms											
q	–	3.49	5.25	1.11	4.14	–	1.87	3.84	2.91	4.58	4.02
or	3.37	1.77	3.55	0.71	1.77	2.19	0.89	4.02	1.42	1.42	1.48
ab	23.01	21.74	21.83	22.59	24.45	11.76	20.98	16.41	22.51	22.59	22.68
an	30.67	24.25	29.35	27.50	33.10	35.27	26.44	25.28	23.67	22.59	23.53
di	12.87	14.40	10.62	19.49	–[b]	0.56	8.63	3.71	20.29	14.76	16.39

TABLE 5 – *Continued*

	250A-26-6, 45-47 cm	251A-30-1, 140-145 cm	251A-31-1, 39-41 cm	251A-31-4, 29-31 cm	253-24-1, 84-85 cm	253-58-1, 2-7 cm	254-36-3, 95-97 cm	254-38-1, 115-117 cm	256-9-3, 45-47 cm	256-10-2, 87-90 cm	256-11-3, 110-113 cm
hy	10.28	13.51	7.70	20.54	22.90	21.39	20.56	24.55	17.63	18.97	18.31
ol	9.80	–	–	–	–	15.64	–	–	–	–	–
mt	2.47	9.81	11.67	2.47	3.68	4.68	8.10	10.44	4.44	5.15	5.19
il	2.77	2.79	3.38	3.04	1.77	1.31	4.69	3.00	4.75	4.84	4.71
ap	0.59	0.38	0.64	0.35	0.78	0.19	0.61	0.40	0.59	0.52	0.61
cc	2.00	4.80	3.48	0.52	3.68	0.86	2.75	0.61	0.64	2.21	0.89

Note: The analyses in this table are revisions of those in Kempe (1973a).

[a]Analysts: C. J. Elliott and V. K. Din.

[b]Includes cor, 0.18.

[c]Data from Frey et al. (this volume, Chapter 23).

TABLE 6
Chemical Analyses of the Basalts from Site 257

	Sample											
	257-11-2, 82-84 cm	257-12-2, 79-81 cm	257-13-3, 43-44 cm	257-14-2, 78-80 cm	257-14-4, 124-126 cm	257-15-1B, 126-128 cm	257-15-2, 37-39 cm	257-15-2, 122-124 cm	257-16-2, 94-96 cm	257-17-1, 91-93 cm	257-17-3, 26-28 cm	257-17-5, 65-67 cm
SiO_2	49.70	49.12	49.01	48.30	50.42	50.02	49.18	48.31	49.71	47.97	49.24	50.54
TiO_2	1.19	0.86	0.82	0.86	0.99	0.88	0.88	0.89	0.83	0.88	0.94	0.92
$A1_2O_3$	16.42	15.18	14.47	15.08	14.72	16.00	15.05	15.73	17.40	14.32	14.72	14.46
Fe_2O_3	1.71	3.05	2.22	2.91	1.81	2.08	2.37	5.07	2.21	3.70	1.79	1.65
FeO	5.02	4.63	6.04	4.41	8.45	6.12	6.64	4.37	5.87	5.16	6.56	7.96
MnO	0.28	0.20	0.24	0.16	0.19	0.17	0.25	0.22	0.16	0.15	0.17	0.17
MgO	7.97	9.18	8.66	9.05	7.43	7.83	8.78	7.88	7.17	8.08	8.52	8.06
CaO	11.76	11.67	12.51	11.99	11.70	12.59	12.17	10.86	13.01	12.41	12.65	12.25
Na_2O	2.39	2.24	2.05	2.23	2.06	2.07	1.86	2.13	2.00	2.04	2.04	2.02
K_2O	0.12	0.24	0.05	0.41	0.06	0.04	0.11	0.73	0.04	0.45	0.11	0.08
H_2O^+	0.89	1.07	0.74	1.08	0.48	0.40	0.56	1.43	0.65	0.88	0.84	0.63
H_2O^-	1.99	2.74	1.59	2.94	0.73	1.26	1.55	2.53	0.90	2.35	1.68	0.84
P_2O_5	0.20	0.10	0.10	0.09	0.10	0.07	0.08	0.09	0.08	0.11	0.10	0.09
CO_2	0.36	0.41	1.05	1.26	0.32	0.55	0.42	0.42	0.23	1.29	0.77	0.24
Others	0.18	0.14	0.14	0.17	0.11	0.14	0.15	0.15	0.15	0.14	0.13	0.12
Total	100.18	100.83	99.69	100.94	99.57	100.22	100.05	100.81	100.41	99.93	100.26	100.03

TABLE 6 – *Continued*

	257-11-2, 82-84 cm	257-12-2, 79-81 cm	257-13-3, 43-44 cm	257-14-2, 78-80 cm	257-14-4, 124-126 cm	257-15-1B, 126-128 cm	257-15-2, 37-39 cm	257-15-2, 122-124 cm	257-16-2, 94-96 cm	257-17-1, 91-93 cm	257-17-3, 26-28 cm	257-17-5, 65-67 cm
Trace elements (ppm)												
Ti	7134	5156	4916	5156	5935	5276	5276	5336	4976	5276	5635	5515
Ga	25	25	25	30	25	25	25	25	40	25	25	20
Cr	390	200	300	335	165	290	325	360	350	220	220	200
Li	18	16	10	12	7	7	7	8	7	13	13	9
Nb	<50	<50	<50	<50	<50	<50	<50	<50	<50	<50	<50	<50
Ni	120	180	140	150	115	130	130	130	115	150	160	100
Cu	17	75	38	50	15	15	25	95	17	88	75	12
V	300	310	310	330	330	310	310	310	290	290	290	330
Zn	90	110	90	90	110	100	90	95	80	200	90	90
Zr	150	100	100	100	100	100	100	50	100	75	100	100
Y	40	50	50	25	50	50	40	25	50	25	25	50
Sr	170	85	75	100	70	65	70	70	75	85	85	75
Pb	–	< 5	10	< 5	–	–	< 5	25	–	< 5	< 5	–
Ba	25	40	40	150	25	10	⩽10	⩽10	40	⩽10	⩽10	25
Rb	< 5	< 5	< 5	< 5	< 5	< 5	< 5	< 5	< 5	< 5	< 5	< 5
Norms												
q	1.45	0.82	1.84	0.72	2.73	2.30	1.29	2.44	1.84	2.39	1.01	1.80
or	0.71	1.42	0.30	2.42	0.36	0.24	0.65	4.31	0.24	2.66	0.65	0.47
ab	20.22	18.95	17.34	18.87	17.43	17.51	15.74	18.02	16.92	17.26	17.26	17.09
an	33.73	30.66	30.14	29.93	30.75	34.25	32.40	31.21	38.39	28.59	30.69	30.16
di	16.84	19.06	19.81	16.67	20.13	19.58	19.99	15.34	19.51	19.22	21.42	23.21
hy	18.15	18.75	20.39	19.21	21.40	18.44	21.48	15.17	16.32	16.22	20.21	20.82
ol	–	–	–	–	–	–	–	–	–	–	–	–
mt	2.48	4.42	3.22	4.22	2.62	3.02	3.44	7.35	3.20	5.36	2.60	2.39
il	2.26	1.63	1.55	1.63	1.88	1.67	1.67	1.69	1.58	1.67	1.79	1.75
ap	0.47	0.24	0.24	0.21	0.24	0.17	0.19	0.21	0.19	0.26	0.24	0.21
cc	0.82	0.93	2.39	2.87	0.73	1.25	0.95	0.96	0.52	2.93	1.75	0.55

Note. The analyses in this table are revisions of those in Kempe (1973a).

[a]Analysts: C. J. Elliott and V. K. Din.

basalt from Site 250 is a low-alumina type, if a dividing value of 16.4% Al_2O_3 is taken. The samples from Site 251 are also very low in Al_2O_3. The samples from Site 253 are high (flow) and low ("basement"), while both analyses of the highly altered basalt from Site 254 are exceptionally low. The same applies to the three somewhat altered samples from Site 256 (average Al_2O_3, 13.2%), while all but two of those from Site 257 are low-alumina varieties. There is some correlation with the presence or absence of phenocrysts, as suggested by Miyashiro et al. (1969). Of the high-alumina samples, Site 253 (flow) and one or two of the Site 257 samples, plagioclase (and pyroxene) phenocrysts are present in Core 14, Site 257, and olivine in the Site 253 flow, one of the two analyzed rocks with the highest content of Al_2O_3. However, the porphyritic "basement" basalt from Site 253 and several highly porphyritic rocks from Site 257 are low-alumina types. Plotted against CaO (Figure 5) the Leg 26 Al_2O_3 values for the fresher rocks are similar to those of Leg 15, except vor those from Site 256 which are low in both components. This adds weight to the observation of Bence et al. (1973b) that this pair

TABLE 7
Some Comparative Average Basalt Analyses

	Leg 26[a]	Dredged Basalts[b]	Carlsberg Ridge[c]	Island Basalts[d]	Oceanic Tholeiite[e]	Ocean Floor[f]	Modal Tholeiite[g]
SiO_2	49.16	49.53	49.14	47.67	49.94	49.61	50.1
TiO_2	1.63	1.24	1.65	2.66	1.51	1.43	1.4
Al_2O_3	14.86	16.62	16.22	15.72	17.25	16.01	15.8
Fe_2O_3	2.61	2.94	2.70	4.51	2.01	–	–
FeO	7.80	6.08	7.57	7.86	6.90	11.49[h]	8.9[h]
MnO	0.19	0.16	0.20	0.30	0.17	0.18	–
MgO	7.30	7.42	7.62	6.75	7.28	7.84	8.3
CaO	11.10	11.37	10.83	9.68	11.86	11.32	12.2
Na_2O	2.40	2.74	3.02	3.05	2.76	2.76	2.5
K_2O	0.17	0.29	0.18	1.35	0.16	0.22	0.10
H_2O^+	0.91	0.75	0.79	–	–	–	0.16
H_2O^-	1.23	0.62	0.30	–	–	–	–
P_2O_5	0.18	0.11	0.08	0.45	0.16	0.14	–
CO_2	0.51	–	–	–	–	–	–
Total	100.05	99.87	100.30	100.00	100.00	101.00	99.46

[a]Average composition of the fresh basalts from Leg 26 (from Tables 5 and 6)
[b]Average of twenty published analyses of basalts dredged from the southern Indian Ocean (Korzhinsky, 1962 [1 analysis]; Engel, Fisher, and Engel, 1965 [8 analyses]; Bezrukov et al., 1966 [2 analyses]; Hekinian, 1968 [4 analyses]; Fisher et al., 1968 [3 analyses]; and Engel and Fisher, 1969 [2 analyses]).
[c]Average of six basalts from the Carlsberg Ridge (Cann, 1969).
[d]Average of 42 published analyses of 'alkali' basalt from islands of the Indian Ocean (Engel, Fisher, and Engel, 1965).
[e]Average oceanic tholeiite (Engel, Engel, and Havens, 1965).
[f]Mean ocean-floor basalt (Cann, 1971).
[g]Model tholeiite (Hart, 1971).
[h]Total FeO (FeO*).

of components shows (with the pair FeO*-MgO) the most pronounced inter- and intra-site major element differences in the Leg 15 basalts.

Except in the case of highly altered rocks, variation diagrams relating FeO*/MgO to other oxides tend to substantiate the findings of Miyashiro et al. (1969) with the Mid-Atlantic Ridge samples. Figure 6 (a-e) shows the FeO*/MgO ratio plotted against SiO_2, TiO_2, Al_2O_3, FeO* and MgO; and also (Figure 7) FeO* plotted against MgO. Similar but more scattered plots are shown by Na_2O and P_2O_5, both of which oxides increase with increases in the ratio. MnO tends to remain constant, lying (with one exception) in the range 0.11%-0.28%. The most notable points about the plots are the tight grouping of the Site 256 analyses as compared with those from Site 257, and the low silica content, relative to the FeO*/MgO ratio of basalts from Site 250 and the Site 256 group. This is due to the low silica at Site 250 and low magnesia at Sitw 256 (Figure 6a). Both Site 256 and Site 257 analyses group closely in the SiO_2 versus total alkalis plot (Figure 8). There appears to be no systematic correlation between MgO and TiO_2 contents (Hekinian, 1968), but in general, MgO decreases with increasing SiO_2 (Miyashiro et al., 1969).

The Na_2O/K_2O ratio for Cann's (1971) mean ocean-floor basalt is 12.5. The Leg 26 ratios for average fresh rocks are:

Site 250	4.8
Site 251	22.3
Site 253 (flow)	9.6
Site 256	11.1
Site 257	18.5-51.8

Clearly, Site 250 basalt is atypical and Sites 251 and 257 basalts are extreme, while those from Site 256 are closest to Cann's average value. The altered rocks (Sites 251, 253, 254, and 257) have ratios ranging from 2.9 to 16.5.

Normative Compositions

The normative compositions of the Leg 26 basalts have been calculated without calcite and with Fe_2O_3 content normalized to 1.50% (Table 8), and are plotted (Figure 9) on the triple triangular diagram of Yoder and Tilley (1962) and Muir and Tilley (1964, 1966). It can be seen that many, especially those for Sites 251, 256, and 257, are quartz-normative, i.e. quartz tholeiites. Rather surprisingly, the most olivine-rich (modally and normatively) of all the basalts (apart from the Site 253 "picritic basement") comes from Site 250 (Mozambique Basin).

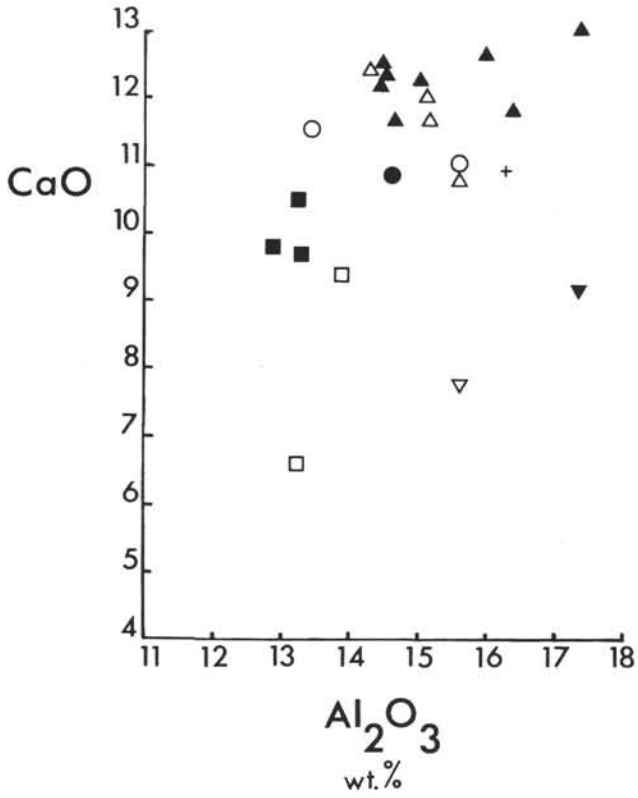

Figure 5. *CaO plotted against Al_2O_3 for the analyzed Leg 26 basalts. (Solid symbols, fresh or fairly fresh basalts; open symbols, altered basalts). Cross, Site 250; circles, Site 251; solid inverted triangle, Site 253 flow; open inverted triangle, Site 253 altered "picritic" basement; open squares, Site 254; solid squares, Site 256; normal triangles, Site 257 (solid, fresh; open, altered).*

Basalt drilled from or near the Mozambique Ridge (Sites 248 and 249), on the other hand, is strongly quartz-normative (Erlank and Reid, in press).

Ocean floor basalts commonly contain normative quartz but this is often due to high Fe_2O_3 contents resulting from weathering or alteration of the basalts. As Fe_2O_3/FeO ratios increase, normative olivine diminishes and is replaced by normative quartz (Kay et al., 1970). Many good examples of this are found in often highly altered rocks sampled by DSDP Leg 16, eastern Pacific, Yeats et al., 1973; Leg 22, Indian Ocean, Hekinian, 1973, 1974a, and 1974b. However, it appears from the recalculated analyses of the highly altered rocks from Site 251 (Section 30-1 and Section 31-1) and Site 254 that loss of 4-5% of silica can, when the degree of alteration is great enough, override oxidation of the FeO to Fe_2O_3 and produce highly olivine-normative rocks. A sequence: fresh→altered→highly altered rocks, yielding quartz-normative→highly quartz-normative→olivine-normative analyses, thus results. Clearly this phenomenon must be taken into account when classifying ocean-bottom basalts: for example, it may well be that the Site 254 basalt is, in fact, quartz-normative when fresh, as indicated by its actual normative composition.

TABLE 8
Normative Compositions on a cc - Free, Fe_2O_3 = 1.50%, Basis

Sample (Interval in cm)	*qz*	*di*	*hy*	*ol*
250A-26-6, 45-47	–	17.37	3.44	13.54
251A-30-1, 140-145	–	26.00	0.56	14.63
251A-31-1, 39-41	–	19.45	2.76	12.16
251A-31-4, 29-31	0.57	20.71	20.42	–
253-24-1, 84-85	0.64	7.83	21.72	–
253-58-1, 2-7	–	2.50	15.49	22.42
254-36-3, 95-97	–	15.17	10.87	12.08
254-38-1, 115-117	–	5.25	26.96	7.92
256-9-3, 45-47	0.77	21.94	20.57	–
256-10-2, 87-90	0.93	20.04	21.35	–
256-11-3, 110-113	1.14	18.64	22.24	–
257-11-2, 82-84	0.72	18.70	17.77	–
257-12-2, 79-81	–	21.38	16.01	3.86
257-13-3, 43-44	–	25.28	18.02	1.06
257-14-2, 78-80	–	23.25	10.21	6.65
257-14-4, 124-126	1.94	21.82	21.32	–
257-15-1B, 126-128	0.89	22.47	18.43	–
257-15-2, 37-39	–	22.26	21.51	0.69
257-15-2, 122-124	–	17.97	14.57	5.77
257-16-2, 94-96	0.73	20.80	17.40	–
257-17-1, 91-93	–	26.16	11.38	4.90
257-17-3, 26-28	–	25.40	17.66	0.95
257-17-5, 65-67	1.30	24.47	20.58	–

Calcite calculated in the norm also increases the possibility of normative quartz. However, if all the iron in the analyses is calculated as ferrous (FeO*) it appears (Figure 9) that the average for 20 basalts dredged from the southern Indian Ocean (Table 7), Cann's (1971) typical ocean-floor basalt, and Hart's (1971) model tholeiite all contain considerably more olivine in the norm than the average for the fresher Leg 26 basalts, and, therefore, plot nearer to the olivine corner. Dredged basalts are often fresher than drilled basalts and therefore contain lower Fe_2O_3/FeO ratios; however, the average Fe_2O_3 content of 2.9% for 20 dredged basalts from the southern Indian Ocean, and the average Fe_2O_3 content of 2.6% for the fresher Leg 26 basalts indicates the reverse. The length of the tie-lines joining the real normative compositions with those recalculated using FeO* will, in general, vary inversely with the degree of freshness of the rock. Nevertheless, it is suggested tentatively that drilled basalts contain less normative olivine, and may more often contain normative quartz, when compared with dredged basalts, nearly all of which plot (Figure 9) as olivine tholeiites (Chayes, 1972). A study of the normative compositions of all published dredged and drilled ocean-floor basalts, calcite-free and normalized to Fe_2O_3 = 1.50% and to FeO*, is in preparation. If it can be shown that drilled ocean-floor basalts are more quartz-rich normatively than dredged samples, it is suggested that drilled, ocean-floor basalts may be structurally deeper and possibly poorer in Al_2O_3 than the olivine tholeiites dredged from the crests and slopes of mid-oceanic ridges. There are indications, also, that some basalts with strong alkaline affinities from the South Atlantic Ocean are quartz-normative (Kempe, 1973b, Kempe and Schilling, 1974). A model to explain

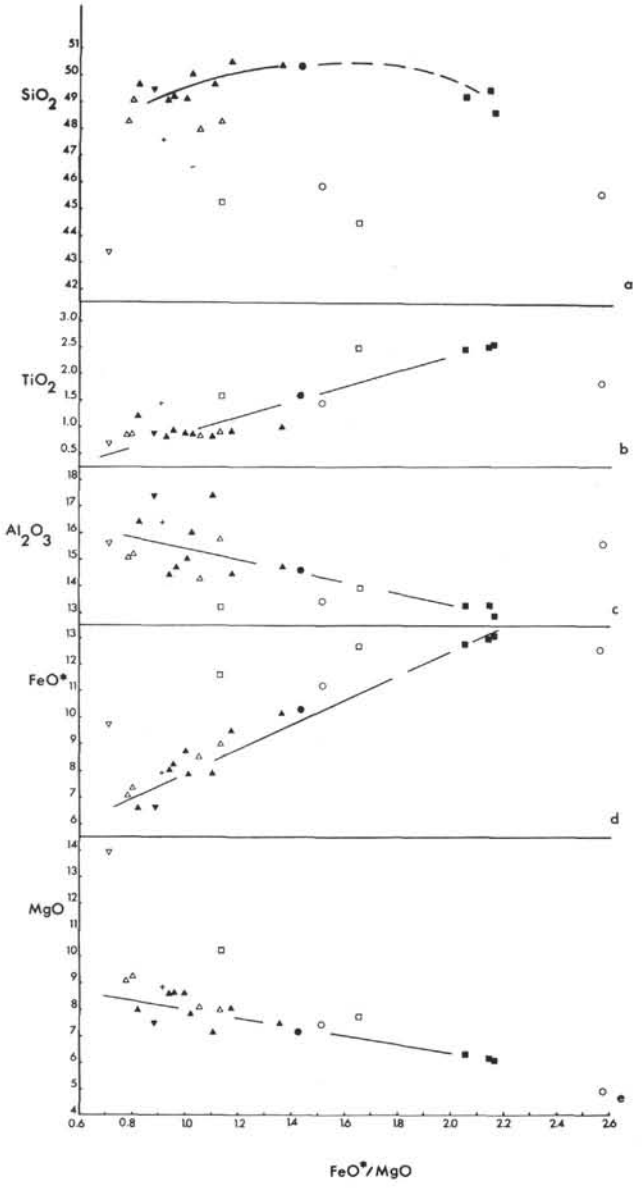

Figure 6. *FeO*/MgO ratio for the Leg 26 basalts plotted against: (a) SiO_2; (b) TiO_2; (c) Al_2O_3; (d) FeO*; and (e) MgO. (FeO* = total Fe as FeO; symbols as in Figure 5.)*

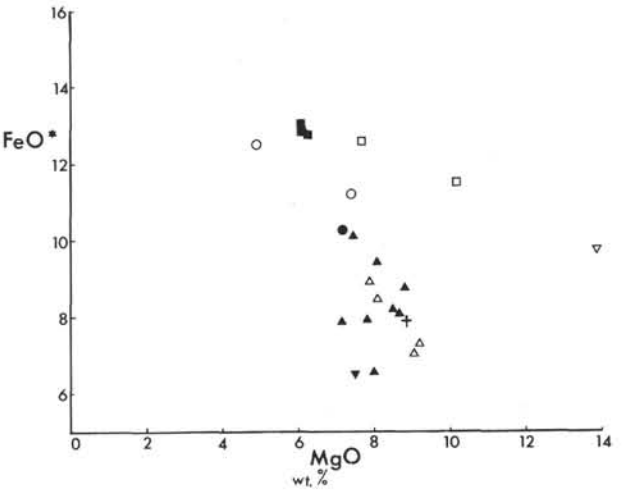

Figure 7. *FeO* vs MgO for the Leg 26 basalts. (Symbols as in Figure 5.)*

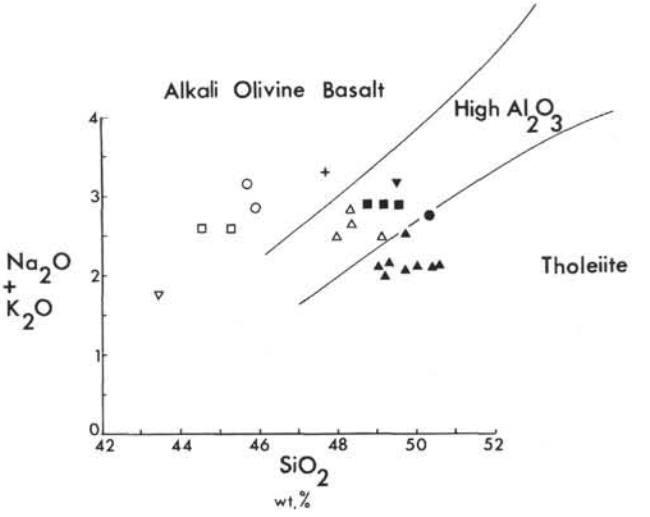

Figure 8. *Total alkalis ($Na_2O + K_2O$) vs SiO_2 for the Leg 26 basalts. (Symbols as in Figure 5.)*

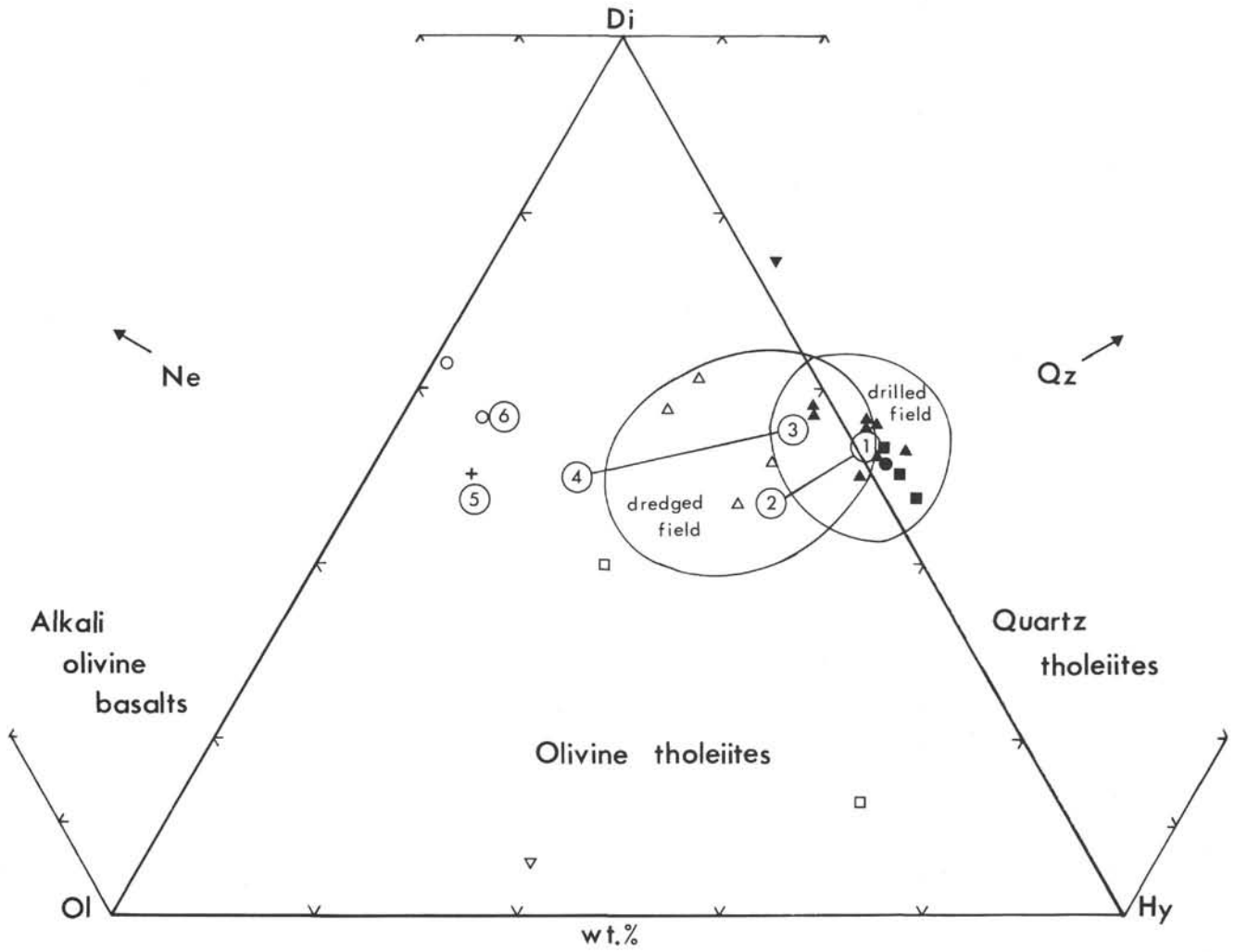

Figure 9. *Triangular plots to show normative compositions of the Leg 26 basalts, normalized on a cc-free, Fe_2O_3 = 1.5% basis (Table 8). Average compositions, using actual normative values: (1) average of the fresh Leg 26 basalts; (2) Leg 26 average recalculated with FeO*; (3) average of 20 analyzed dredged basalts from the southern Indian Ocean (Table 7); (4) average of 20 dredged basalts with FeO*; (5) Cann's (1971) mean ocean-floor basalt, with FeO*; and (6) average of 42 published analyses of "alkali" basalts from islands of the Indian Ocean (Engel, Engel, and Havens, 1965). Suggested drilled and dredged fields are for ocean-floor basalts. (Symbols as in Figure 5.)*

the generation of quartz-normative basalts in two distinct contexts may therefore be required.

The analyses were also plotted (using Fe_2O_3 = 1.50) in the triangular diagram Px(*di*+*hy*)-Ol(*fo*+*fa*)-Pl(*ab*+*an*), used by Miyashiro et al. (1970) to distinguish between OL-tholeiites and PL-tholeiite i.e., those in which olivine and plagioclase phenocrysts, respectively, crystallize first. Obviously, the fresh Sites 251 and 257, the Site 256, and the Site 253 flow basalts must be PL-tholeiites, since they contain no normative olivine. In fact, Site 250 is also just a PL-tholeiite (Figure 10), falling close to the (cotectic) boundary line between the two fields. The picritic Site 253 "basement", the Site 254, and the altered Sites 251 and 257 basalts are OL-tholeiites. The two fields of Miyashiro et al. (1970) are shown and it is interesting that the average of 20 southern Indian Ocean dredged basalts is a PL-tholeiite, falling close to the Leg 26 cluster. There is clearly a strong tendency in the Indian Ocean rocks to be olivine-poor.

The classification used by Hekinian and Aumento (1973) to group the tholeiites dredged from the Gibbs Fracture Zone and the Minia Seamount, near 53°N, North Atlantic Ocean, was also applied to the Leg 26 basalts (Figure 11). There are points of agreement but on the whole it would appear that this type of classification can only be applied to a group of rocks from single, or closely related, localities. For instance, the only rocks from Leg 26 to 4ot as high-alumina plagioclase tholeiites are three of the olivine-normative rocks, from Sites 250, 251, and 253 "basement". Their Al_2O_3 content is fairly high (Table 5) but they contain no large plagioclase phenocrysts. The only rocks that do (Site 257) plot as pyroxene and plagioclase tholeiites, the

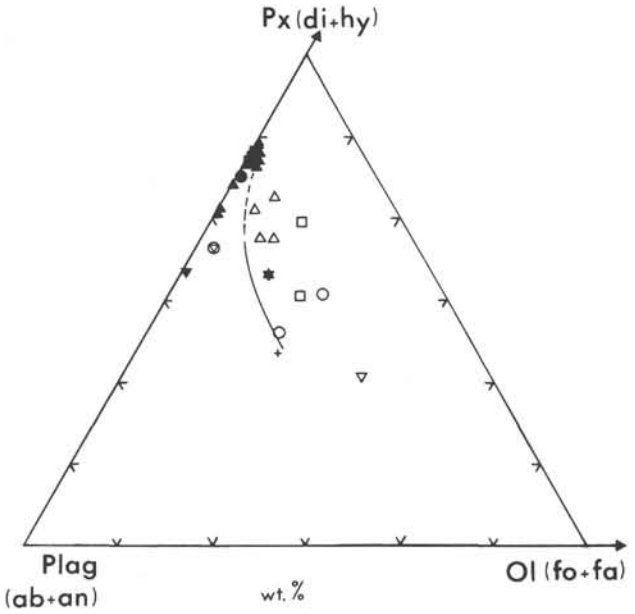

Figure 10. *Leg 26 basalts, normalized on a cc-free, Fe_2O_3 = 1.5% basis, plotted in the normative diagram Px(di+hy) -Op(fo+fa)-Pl(ab+an). The full line represents a cotectic curve (Miyashiro, et al., 1970). Star, a typical average Mid-Atlantic Ridge basalt, and triangle-within-circle, average of 20 dredged southern Indian Ocean basalts (Table 7), both using actual normative values. (Symbols as in Figure 5.)*

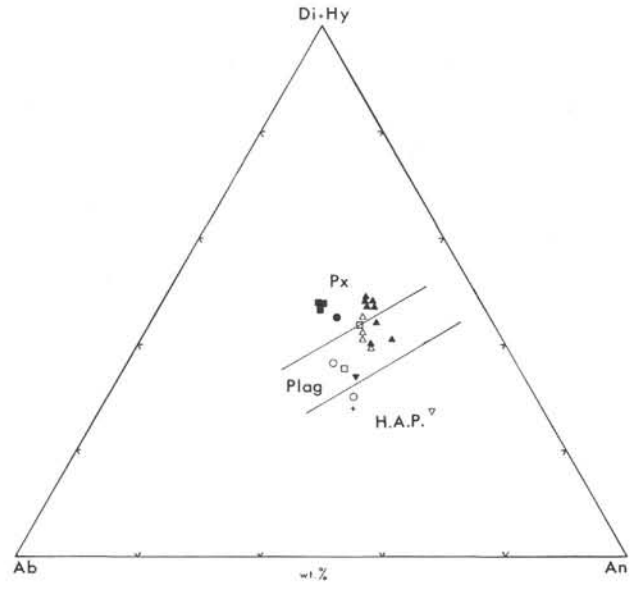

Figure 11. *Leg 26 basalts, normalized on a cc-free, Fe_2O_3 = 1.5% basis, plotted in the normative diagram (di+hy)-ab-an (Hekinian and Aumento, 1973). (Symbols as in Figure 5.)*

porphyritic (An_{88}) samples falling in both areas. Of the remainder, the Site 253 flow, one Site 254, and an altered Site 251 basalt plot as plagioclase, and Sites 251 (fresh) and 256 plot as pyroxene tholeiites: the latter group rightly includes the pyroxene-rich basalt from Site 251. It is interesting to note that the Gibbs-Minia suite of rocks is generally far more quartz-normative than is usually found in rocks dredged from the Mid-Atlantic Ridge.

Crystallization Differentiation

Only recently have data become available to show homogeneity, or lack of it, among oceanic tholeiites when plotted on the FMA diagram. However, Miyashiro et al. (1970) have shown that there may be considerable compositional variation in tholeiites and gabbros dredged from the Mid-Atlantic Ridge, spanning an FeO* component of the order 25%, or 35% if an iron-rich gabbro from *Vema* Cruise 25, Rock Dredge 6, is included (Miyashiro et al., 1970, Table 3, analysis 3). This range more than doubled the range existing before analysis of *Vema's* Dredges 5 and 6 of Cruise 25. Virtually linear correlation is obtained if FeO* is plotted against An (mol.%) in the (modal) plagioclase of the rocks. Unfortunately, no structural parameter is available against which to plot the clearly crystallization-differentiated tholeiites and gabbros, since the samples were dredged across the Mid-Atlantic Ridge and may have originated from any height on the ridge crest above the path of the dredge. Basalts from Leg 16 of the DSDP, taken from the eastern Pacific Ocean, also show considerable FMA variation, especially the six analyses from Site 163 (Yeats et al., 1973). However, no relationship exists between position on the plot and, for example, distance from the East Pacific Rise, although the six Site 163 analyses show linearity and do not form a cluster. It was very fortunate that on Leg 26 basalt was drilled to the extent of 19 and 64.5 meters, respectively, from Sites 256 and 257. This enabled short series of analyses to be carried out on samples from these holes and the results related to the depth below the sediment-basalt contact. The analyses are plotted in Figures 12 (FMA) and 13 (lime-alkali), together with the single analyses for Leg 26 and selected data from the Mid-Atlantic Ridge. Clearly there is a well-defined field for abyssal or tholeiitic basalts and gabbros. In the FMA diagram, the Leg 26 analyses plot between the limits of the average compositions from the Mid-Atlantic Ridge (Miyashiro et al., 1970). The Site 256 basalts plot on the FeO* side of the typical iron-rich gabbros but inside the extremely iron-rich T124 gabbro. Thus, together with this gabbro, a basalt (FET1) from Site 32, Leg 5 (Melson, 1973), and basalts from Leg 9 (Rhodes, 1973), the Site 256 rocks may be among the most highly fractionated (Fe/Mg enriched) of all known ocean-floor basalts (Figure 14).

Although the Site 256 basalts string out parallel to the FeO*-MgO join (the F-M join in Figure 12), variation is too limited for them to be satisfactorily related to depth below the sediment-basalt contact (Figure 15). In the case of the lime-alkali plot (Figure 13), there is clear differentiation away from the calcium-rich corner. The group of 12 analyses from Site 257, however, shows very clear differentiation on both FMA and lime-alkali diagrams and these trends can generally be related to

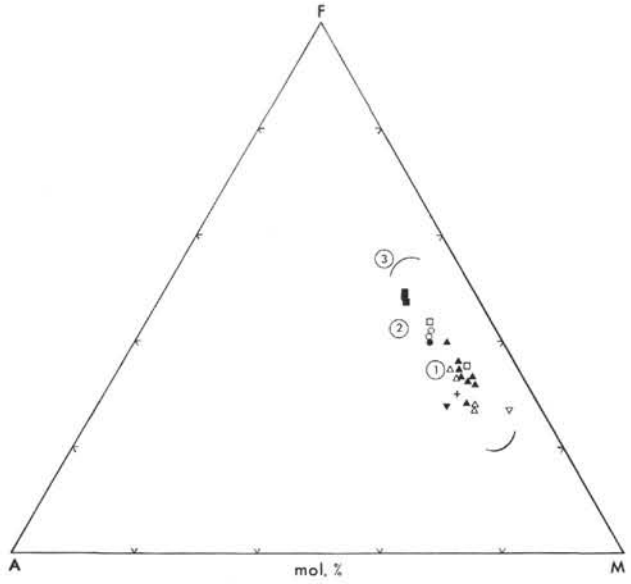

Figure 12. *FMA diagram of the Leg 26 basalts. Brackets enclose area filled by Mid-Atlantic Ridge rocks, including the iron-rich gabbro, of Miyashiro et al. (1970). (1) Average of 20 dredged southern Indian Ocean basalts (Table 7); (2) average of 42 "alkali" basalt analyses from islands of the Indian Ocean (Engel, Engel, and Havens, 1965); and (3) FETI basalt, Site 32, Leg 5 (Melson, 1973b). (Symbols as in Figure 5.)*

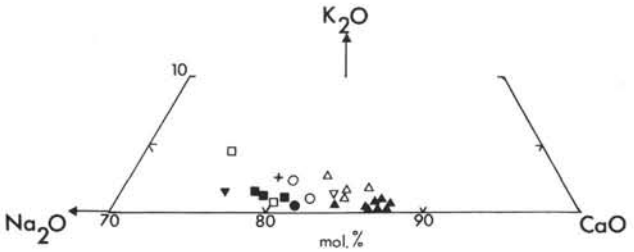

Figure 13. *Lime-alkali diagram of the Leg 26 basalts. (Symbols as in Figure 5.)*

depth below the contact (Figures 16 and 17). Age determinations of the basalts from Site 257 have shown them to be flows separated by an erosion interval in Core 15 (Table 1). There is no question, therefore, of successive injection as a series of sills. Hence it is very remarkable that the Site 257 basalts, although differentiating from the calcic to he sodic corners of the lime-alkali diagram in accordance with normal fractionation, enrich in iron downwards and not upwards as is usual in a series of (?stratified) flows. Conversely, in Site 256, although no very clear iron-enrichment trend can be related to depth, the indication is that it occurs upwards in the sequence. Lime-alkali enrichment does the reverse, trending towards calcium-enrichment upwards. Clearly more analyses are required to verify these results, but at this stage it appears that crystallization differentiation, related to the structural position of the flow (i.e., depth

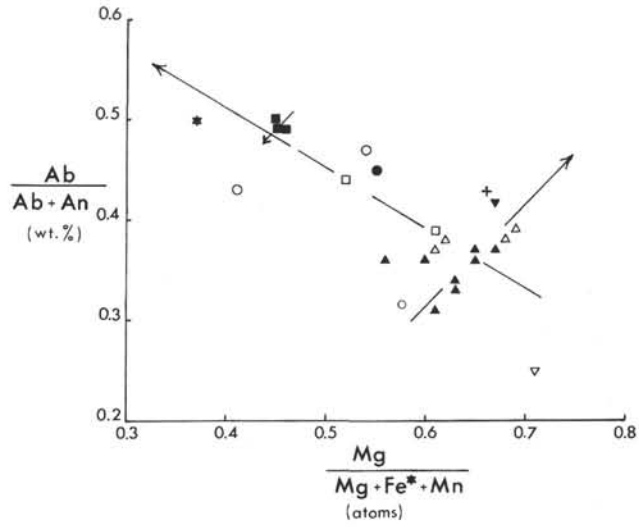

Figure 14. *Fractionation diagram Ab(Ab+An) vs Mg(Mg+Fe*+Mn) for the Leg 26 basalts (after Rhodes, 1973). The long arrow indicates general fractionation trend of tholeiitic basalts. Shorter arrows indicate upwards fractionation trends at Sites 256 and 257. Star, FETI basalt, Site 32, Leg 5 (Melson, 1973b). (Symbols as in Figure 5.)*

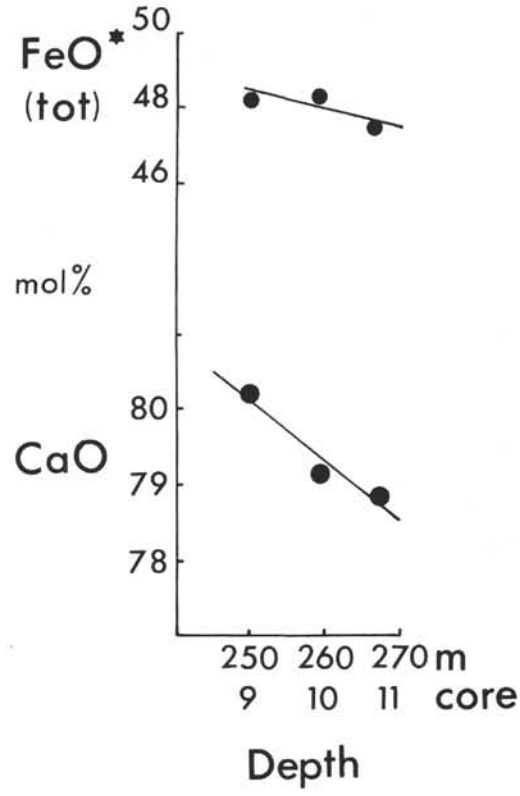

Figure 15. *FeO* from the FMA diagram, and CaO from the lime-alkali diagram, for Site 256 basalts plotted against depth below sediment-basalt contact.*

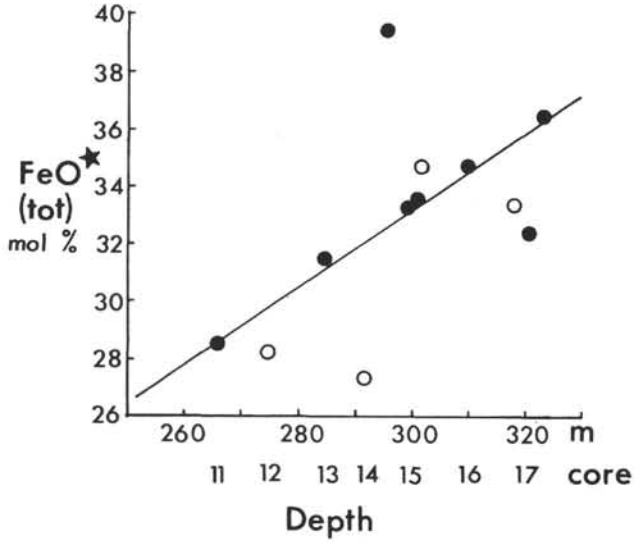

Figure 16. *FeO* from the FMA diagram for Site 257 basalts plotted against depth below sediment-basalt contact. Solid circles, fresh basalts; open circles, somewhat altered basalts.*

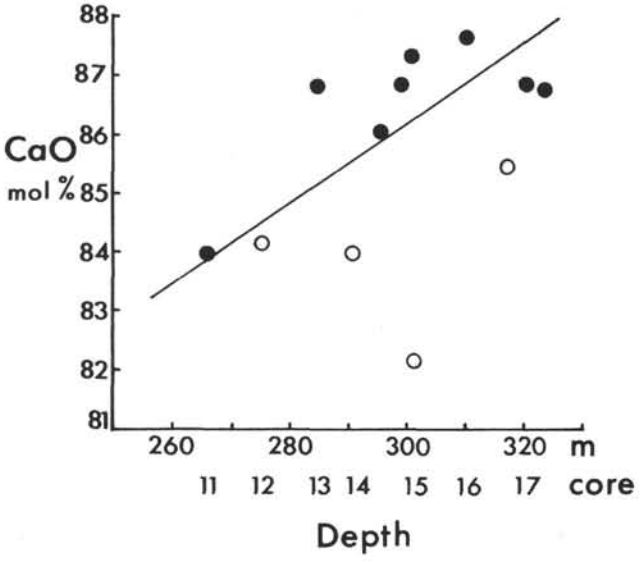

Figure 17. *CaO from the lime-alkali diagram for Site 257 basalts plotted against depth below sediment-basalt contact. Solid circles, fresh basalts; open circles, somewhat altered basalts.*

below the sediment-basalt contact), is not straightforward. A tentative model to account for this is discussed below.

Trace Elements

Consideration of the trace elements in the basalts (Tables 5 and 6) shows a fairly wide range in most elements. However, comparison with major, minor, and trace element concentrations typical of ocean floor (tholeiite) basalts and alkali basalts (from seamounts and islands) (Engel, Engel, and Havens, 1965) shows strong evidence of an ocean-floor-basalt origin for all the analyzed samples, with the possible exception of Site 250, which shows calc-alkaline affinities. The levels of potassium, strontium, and barium and, so far as is known, rubidium, are generally within the ranges given by Hart (1969, 1971), as are rocks dredged from the Mid-Indian Ocean Ridge (Subbarao and Hedge, 1973, based on many of the rocks used also in the calculation of the average composition given in Table 7, analysis B). The three analyses from Site 256 show similar trace-element suites in each case, as they do for the major elements. The 12 from Site 257 are less homogeneous; for instance Core 257-11, the highest Site 257 sample analyzed, is exceptionally rich in strontium. The magnesium-rich picritic "basement" from Site 253 shows the most extreme trace element values, with enrichment in the "basic" elements nickel and chromium, and depletion in vanadium and barium.

The TiO_2 values are interresting, ranging as they do between 0.69% (Site 253 "basement") and 2.55% (Site 256). Rather surprisingly, the Site 250 basalt has a relatively low TiO_2 content (1.5%), despite the nature of its pyroxene (Al-Ti-rich salite). The fresh Site 251 basalt has a typical content of TiO_2 (1.6%), while the two Ninetyeast Ridge sites have 0.9% and 0.7%, and 2.5 and 1.6% respectively. Finally, the remarkable difference (nearly a factor of three) between the titania content of the Site 256 (average 2.51%) and Site 257 (0.96%) basalts serves to emphasize that despite strong resemblances (e.g., normative and pyroxene compositions, Figures 5 and 12), there are considerable differences, associated with crystal fractionation, between the basalts from the two Wharton Basin sites. Plotted against P_2O_5, the titanium enrichment of the Site 256 basalts results in their falling in the ocean-island tholeiite field, while the remainder plot as ocean-ridge basalts.

The values for the Leg 26 basalts of the trace-element suite investigated by Cann (1970) and Pearce and Cann (1973) were considered. Cann (1970) named the elements rubidium, strontium, yttrium, zirconium, and niobium, and also potassium and titanium, as valuable in defining ocean-floor basalts. Of these, rubidium, strontium, and potassium are affected by alteration processes (deuteric alteration and weathering), while yttrium, zirconium, niobium, and titanium appear to be unaffected. Using the scheme of Pearce and Cann (1973), the basalts were first plotted on a Ti-Zr-Y diagram. No within-plate basalts (WPB) were indicated but Site 250 (and possibly the Site 253 flow) were shown to lie on the border of the calc-alkali basalt field, the remainder being ocean-floor basalts. Reference to the Ti-Zr-Sr diagram (Figure 18) again indicated a calc-alkaline affinity for Site 250 and the remaining fresh rocks to be ocean-floor basalts; of the altered samples (tested on the Ti-Zr plot), the Site 253 flow again falls in the calc-alkaline field. In a Zr-Sr plot the Leg 26 basalts, especially Site 257, have fairly typical ocean-ridge-basalt values although Site 256 and others are somewhat enriched in zirconium relative to strontium.

In Figure 19 strontium is shown plotted against K_2O for the fresher Leg 26 basalts. The four main types of oceanic basalt of Hart et al. (1970) are also shown. It is

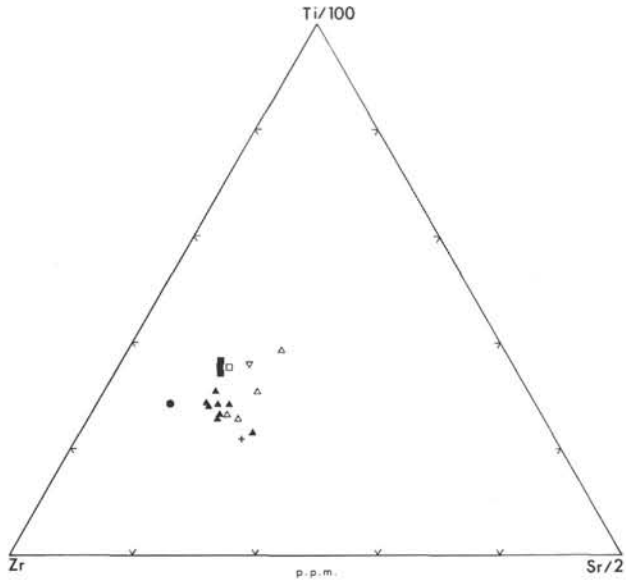

Figure 18. *Leg 26 basalts plotted in the triangular diagram Ti/100-Zr-Sr/2 (Pearce and Cann, 1973). Sites 250, and 253 flow basalts lie on the calc-alkali border: the remainder plot as ocean-floor basalts. (Symbols as in Figure 5.)*

interesting that the Site 250 basalt again stands out from the remainder and that the Sites 251 and 257 basalts extend the range of ocean-floor basalts by being depleted in both elements. The Ni/Cr ratio varies between 1.0 (Site 256) and 2.1 Site (257). This field is close to that given for oceanic tholeiites by Gast (1968) but shows some depletion in chromium. If plotted against MgO, nickel shows similar concentrations in the Leg 26 samples to basalts from the Mid-Atlantic Ridge and East Pacific Rise (Kay et al., 1970) but with some enrichment in nickel in some cases, including Site 256. The highly fractionated Site 256 basalts practically double the range for oceanic basalts when FeO*/MgO is plotted against nickel and chromium (Figure 20); those from Site 257 have values typical of PL-tholeiites (Thompson et al., 1972).

PHASE CHEMISTRY

Electron-microprobe analyses were carried out on pyroxene and plagioclase feldspar crystals from one analyzed rock from each of Sites 250, 251, 254, and 256 (Core 10). In the case of Site 257, analyses were made from five rocks, and, in the case of Cores 14 and 16, from both phenocrysts and groundmass crystals. Average and selected individual analyses are reported in Tables 9-12; all the analyses are plotted in Figures 21 and 22 in order to show the range of compositions within a single rock section.

Probe analyses, in which total iron is reported as FeO, were made using a Cambridge Instruments Geoscan at an accelerating voltage of 15 kv and a specimen current of 0.7×10^{-7} amps. Analyzed silicates, oxides, and metals were used as standards. At least five grains each of pyroxene and feldspar were analyzed for each section, a minimum of 12 spot counts being taken per grain. Results were corrected after the method outlined in Sweatman and Long (1969) using the BM-IC-NPL computer program (Mason et al., 1969). The molecular proportions of the end members were calculated by hand, with random checks for stoichiometric proportions.[2]

Pyroxenes

The pyroxenes from Sites 251, 254, and 256 form a group within the augite field, typical of tholeiitic basalt pyroxenes (Muir and Tilley, 1964, Figure 5). They are slightly more iron rich than the center points of Groups 1 and 2 of pyroxenes from Leg 16 (Yeats et al., 1973). It is interesting to note the spread of analyses from Site 256 and, to a lesser extent, from Site 251. Analyses from Sites 254 and 250 bunch closely together. An average of three analyses and one extreme analysis are reported for Sites 256 and 251 pyroxenes; the extreme analysis is given only in case any significance becomes apparent later. Most compositions are unremarkable. The Al_2O_3 content is fairly constant at around 2-4% (with one exception), that of Na_2O constant at ~0.2-0.3%. There is some degree of correlation between atomic calcium percentage, which increases with alkali and decreases with tholeiitic, basalt affinity, and degree of quartz-normativeness (positive if quartz-normative, negative if olivine-normative).

The two most interesting pyroxene types come from Sites 250 and 257. The former is very homogeneous and rather alkaline (Figure 21a), falling within the salite field and having high (2.1%) contents of TiO_2 (which is reflected in its strong "titanaugite" clove-coloration) and Al_2O_3 (6.2%), twice the level of the other analyzed samples and well above those from Leg 16 (Yeats et al., 1973). It thus correlates well with the composition of the host rock which is relatively rich in K_2O (0.6%) and contains 10% normative olivine. The pyroxenes from Site 257 (Figure 21b) show a sharp division between the groundmass and phenocrysts. The former fall close to the average Group 2 pyroxene from Leg 16 and level (in terms of iron) with the phenocrysts from the Discovery Tablemount alkali basalt, in the South Atlantic (Kempe and Schilling, in press). They also lie very close to the phenocrystic pyroxene from the Namawale Bay tholeiitic picrite basalt of Hawaii (Muir et al., 1957). The main interest, therefore, lies in the fact that some of the phenocrystic pyroxenes, somewhat enriched in Cr_2O_3, lie in the endiopside field, wherein fall the clinopyroxenes from ultramafic inclusions in basalts (Ross et al., 1954), and the single point where phenocryst-groundmass pyroxene tie-lines from alkali, intermediate, and tholeiitic basalts, extrapolated back towards the Di-En join, tend to meet. It was suggested (Kempe and Schilling, in press) that pyroxenes from this endiopsidic field are "primitive", mantle-derived pyrox-

[2]R. F. Symes and J. C. Leverton, Department of Mineralogy, British Museum (Natural History), London.

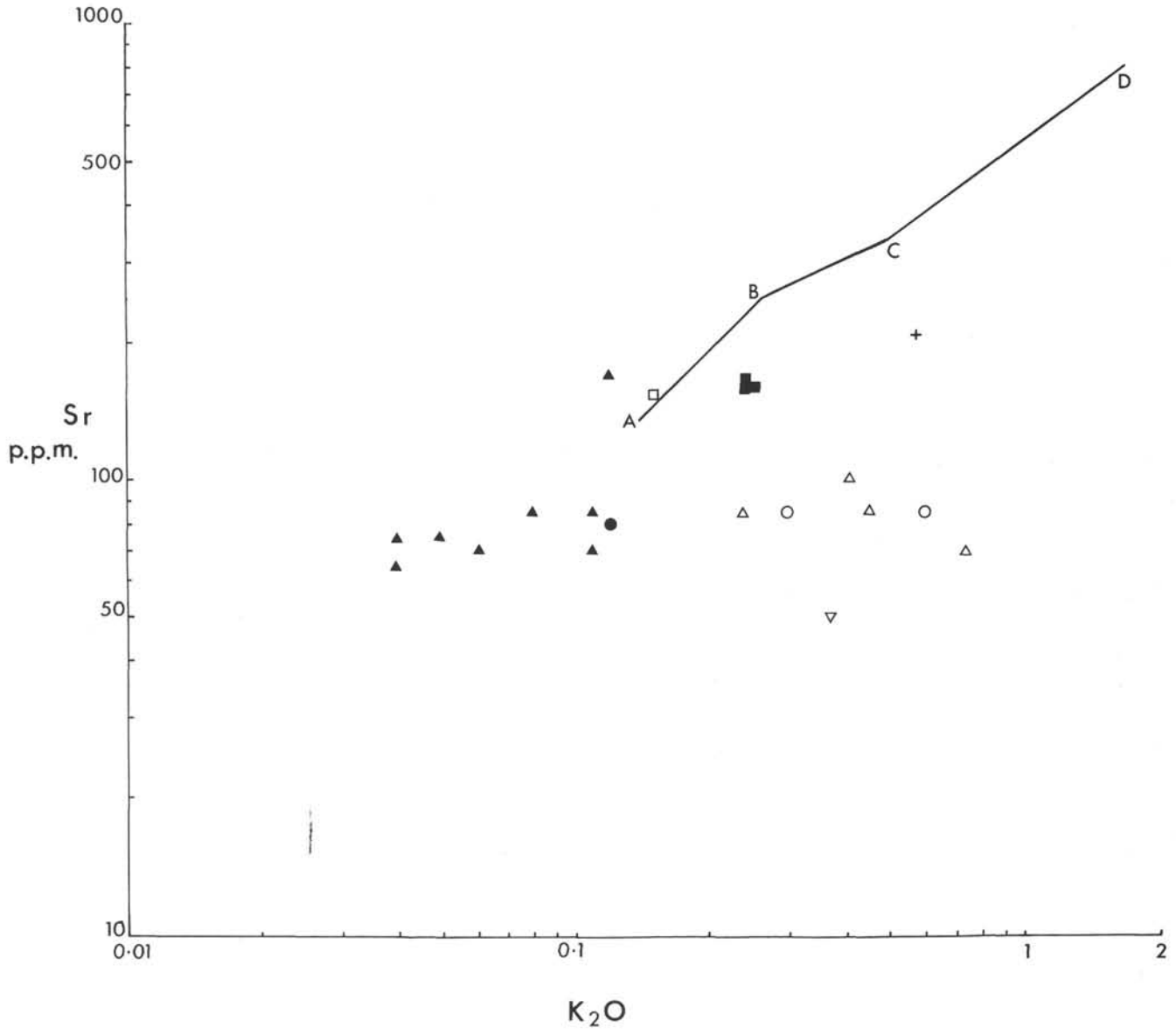

Figure 19. *Sr vs K_2O plot for the Leg 26 basalts (after Hart et al., 1970, Table 2). A, ocean floor basalt; B, low-K tholeiite; C, tholeiite; D, alkali basalt. (Symbols as in Figure 5.)*

enes. Similar endiopsidic pyroxenes but with longer, more pronounced fractionation trends, occur in basalts from the Caribbean (Leg 15) and Central Pacific Basin (Leg 17) (Bence et al., 1973a, b). The compositional range between phenocrysts ($Fe_{11.5}$) and groundmass (Fe_{22}) in the Core 16 pyroxenes is remarkable.

Plagioclase Feldspars

The feldspars (Tables 11, 12, and Figure 22) from the analyzed Leg 26 basalts also show a considerable range in composition (An_{55-91}). By comparison, the feldspars from Leg 15 range from An_{50-88} (Bence et al., 1973b); those from Leg 16 (Yeats et al., 1973, p. 632) from An_{50-79}; and those from Leg 17 (Bence et al., 1973a) are never more calcic than An_{78}. The Leg 26 labradoritic feldspars are rather low in SiO_2, the whole range of which extends from 46-54%, but otherwise are chemically unremarkable. They consistently show normal zoning, from more calcic cores (An_{88-91}) to more sodic rims (An_{63-74}). Unfortunately, Fe_2O_3 and MgO were not determined on these feldspars for comparison with the determinations from Legs 15 and 16. With the exception of the feldspar from Site 257, the feldspar from Site 250 is the most calcic of Leg 26: An_{74}. Otherwise, the interest lies mainly, as with the pyroxenes, in the plagioclases from Site 257. The groundmass is typically An_{73}, but the average phenocryst composition is An_{87}, some crystals reaching An_{90}, and the calcic cores An_{91}. These are extremely calcic for basalt feldspars. The calcic cores of phenocrysts from the PL-tholeiites (*Vema*, Cruise 25, Rock Dredge 1, Mid-Atlantic Ridge: Miyashiro et al.,

TABLE 9
Pyroxene Analyses: Sites 250, 251, 254, 256

	Site 250[a]	Site 251	Site 251[b]	Site 254[c]	Site 256	Site 256[b]
SiO_2	48.14	50.41	50.43	49.50	51.01	50.97
TiO_2	2.07	1.14	1.14	1.80	1.03	1.03
Al_2O_3	6.18	3.26	3.38	3.23	2.82	2.93
Cr_2O_3	0.17	0.24	0.24	0.28	0.33	0.33
FeO*	6.84	9.79	10.89	10.76	8.62	10.51
MgO	13.74	14.98	15.63	13.74	16.64	16.74
CaO	22.52	20.12	18.76	19.86	19.37	16.76
Na_2O	0.31	0.36	0.36	0.31	0.31	0.31
Total	99.97	100.30	100.83	99.48	100.13	99.58
Mg	40.7	43.5	44.4	40.4	47.0	48.3
Fe	11.4	15.5	17.4	17.7	13.7	17.0
Ca	47.9	41.0	38.2	41.9	39.3	34.7

Note: Analysts: R. F. Symes and J. C. Leverton (by electron microprobe).
[a]Average of four.
[b]Average of three.
[c]Average of two.

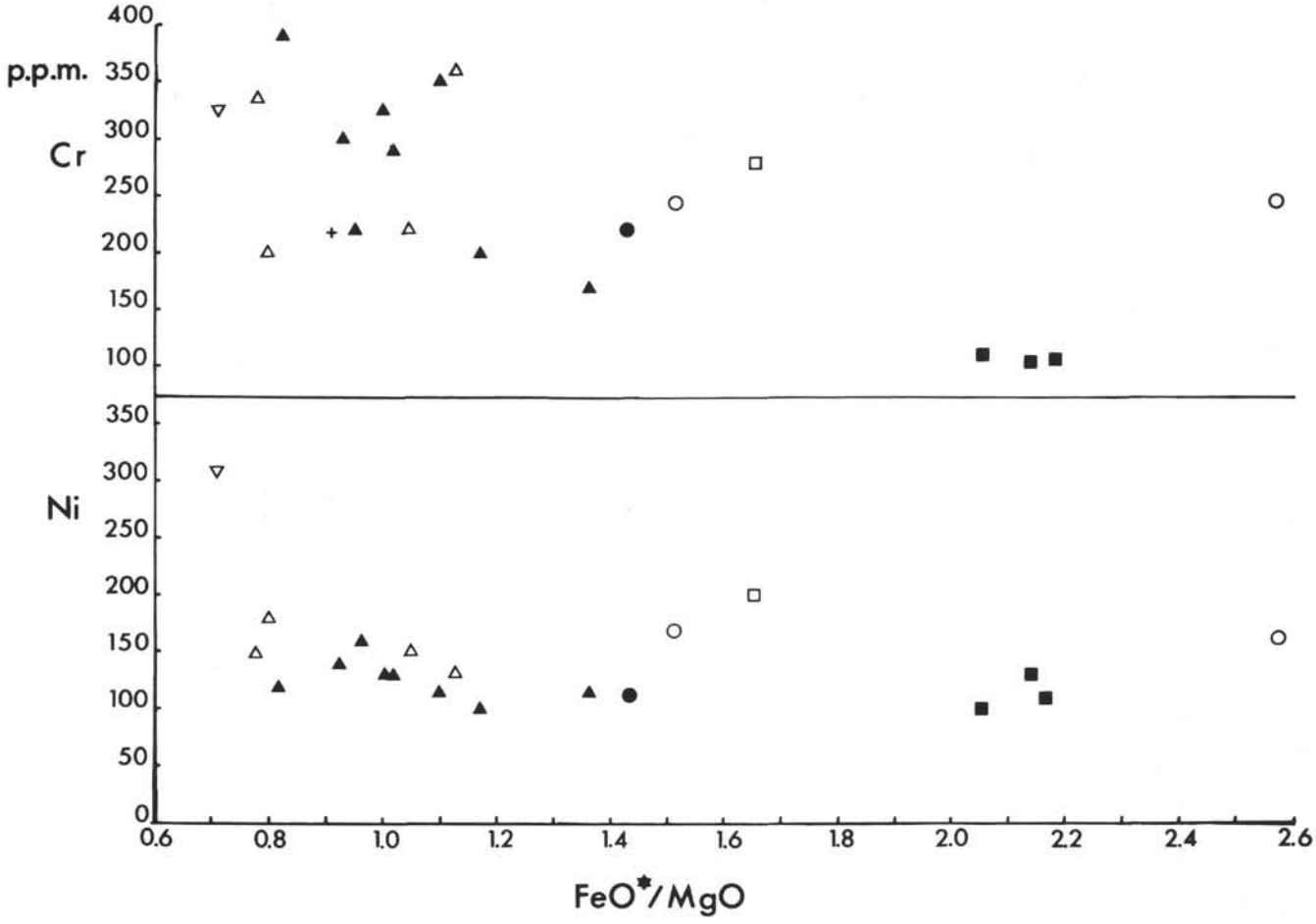

Figure 20. *FeO*/MgO ratio plotted against Ni and Cr for the Leg 26 basalts.*

TABLE 10
Pyroxene Analyses: Site 257 Sections

	Core-Section							
	11-2[a]	11-2	14-4 phenocryst[a]	14-4 groundmass	15-1B[a]	16-2 phenocryst[a]	16-2 groundmass	17-5[b]
SiO_2	51.25	52.40	53.10	52.25	51.98	50.67	52.92	53.06
TiO_2	0.64	0.41	0.17	0.32	0.51	0.68	0.65	0.93
Al_2O_3	3.34	1.92	2.09	2.74	3.43	4.24	2.25	3.14
Cr_2O_3	0.75	0.19	0.53	0.00	0.36	0.33	0.00	0.19
FeO*	5.30	7.08	4.96	7.19	6.30	7.06	13.73	6.46
MgO	17.30	18.43	18.62	17.55	18.04	15.94	16.22	17.46
CaO	20.01	17.77	20.09	18.52	18.17	20.23	15.08	19.92
Na_2O	0.18	0.15	–	–	0.18	0.22	0.13	0.18
Totals	98.77	98.35	99.56	98.57	98.97	99.37	100.98	101.34
Mg	50.0	52.4	52.0	50.3	52.1	46.3	46.7	49.4
Fe	8.5	11.3	7.7	11.6	10.2	11.5	22.2	10.2
Ca	41.5	36.3	40.3	38.1	37.7	42.2	31.1	40.4

Note: Analysts: R.F. Symes and J.C. Leverton (by electron microprobe).
[a]Average of two
[b]Average of three

TABLE 11
Plagioclase Feldspar Analyses: Sites 250, 251, 254, 256

	Sites						
	250[a]	250	251	251	254[a]	256[a]	256
SiO_2	49.40	50.27	51.64	52.67	50.79	53.09	53.51
Al_2O_3	31.75	31.56	29.86	28.53	29.67	28.24	27.37
CaO	14.90	14.88	13.79	12.99	13.62	12.27	11.76
Na_2O	2.77	3.17	3.39	4.09	3.51	4.50	5.24
K_2O	0.12	0.13	0.04	0.04	0.14	0.10	0.13
Totals	98.94	100.01	98.72	98.32	97.73	98.20	98.01
Ab	25.0	27.7	30.8	36.2	31.5	39.5	44.3
An	74.3	71.6	69.0	63.6	67.7	59.9	55.0
Or	0.7	0.7	0.2	0.2	0.8	0.6	0.7

Note: Analysts: R. F. Symes and J. C. Leverton (by electron microprobe).
[a]Average of three.

1970; Shido et al., 1971, p. 259) are only An_{82-85}, although xenocrysts from basalts and olivine-enriched dolerite, with average compositions of An_{88}, have been reported from the rift zone of the Mid-Atlantic Ridge at 45°50'N (Muir and Tilley, 1964). It is apparent that extremely calcic plagioclases (generally bytownites) are more common in ocean floor than in other basaltic lavas: nevertheless, such feldspars are usually found only in plutonic rocks. As in the pyroxenes, the compositional range can be surprising: Core 15 contains feldspars of both An_{88} and An_{70}. Even more notable is the fact that the highly calcic feldspars from Site 257 come from the same ocean-floor feature (the Wharton Basin) as the least calcic (An_{55-60}), from Site 256.

SUMMARY AND DISCUSSION

The oceanic tholeiite basalts from Leg 26 derive from a variety of environments, as their bulk chemistry and mineral chemistry shows. These environments are summarized as follows:

Site 250

The basalt is fairly fresh and notable for the highest K_2O of all the unaltered analyzed samples; it is olivine-normative, a character it shares only with he Ninetyeast Ridge (and altered) basalts. It contains a calcium- and aluminum-rich titaniferous pyroxene (salite) and, with Site 257, the most calcic groundmass plagioclase. The rock shows chemical affinities with the calc-alkaline

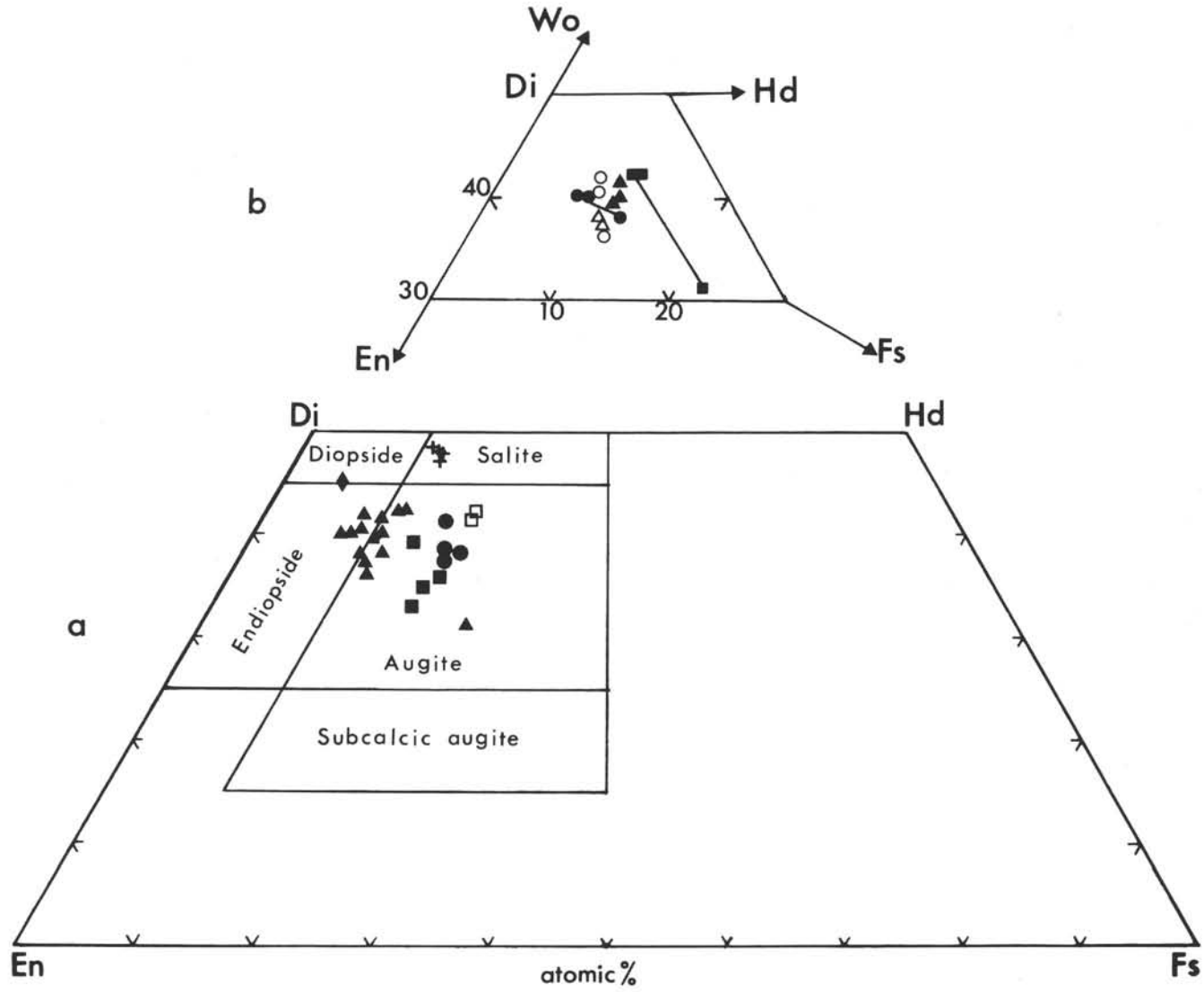

Figure 21. *(a) Pyroxene compositions from the Leg 26 basalts from Sites 250, 251, 254, 256, and 257 (see Tables 3, 9, and 10). (Symbols as in Figure 5.) Diamond, point where pyroxene trend lines from alkali, intermediate and tholeiite basalts intersect, of endiopsidic composition (Kempe and Schilling, in press). (b) Pyroxene compositions from Site 257. Open circles, Core 11; solid circles, Core 14; open triangles, Core 15; solid squares, Core 16; solid triangles, Core 17 (Tables 3, 10). Tie-lines join phenocryst to groundmass compositions for Cores 14 and 16.*

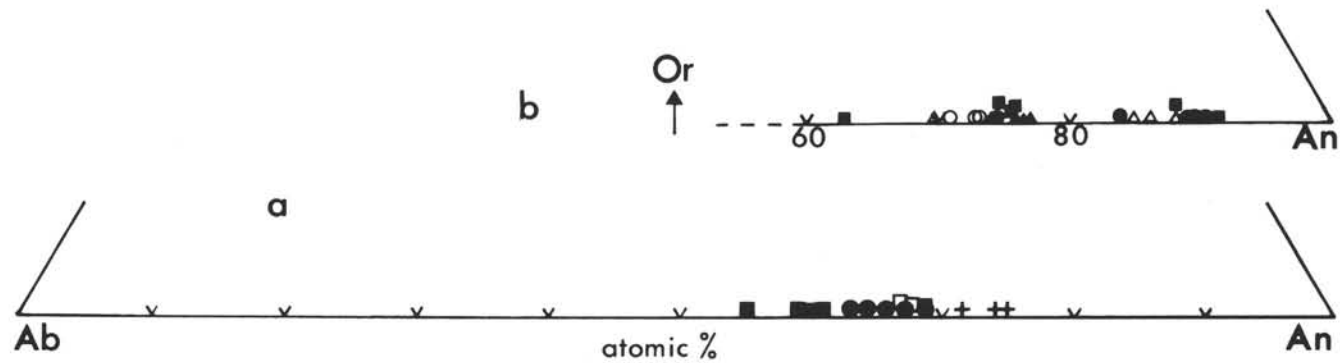

Figure 22. *(a) Plagioclase compositions from the Leg 26 basalts from Sites 250, 251, 254, and 256 (see Tables 3 and 11). (Symbols as in Figure 5.) (b) Plagioclase compositions from Site 257. Open circles, Core 11; solid circles, Core 14; open triangles, Core 15; solid squares, Core 16; solid triangles, Core 17 (Tables 3 and 12).*

TABLE 12
Plagioclase Feldspar Analyses: Site 257

	Core – Section											
							16-2					
							Phenocryst		Phenocryst		Ground-	
	11-2[a]	14-4 Pheno-cryst[a]	14-4 Pheno-cryst	14-4 Ground-mass	15-1B[a]	15-1B	Core	Rim	Core	Rim	mass[b]	17-5[c]
SiO_2	50.52	46.01	47.43	49.18	47.53	51.19	46.07	53.70	46.51	49.50	49.62	49.57
Al_2O_3	29.95	34.07	32.79	30.46	32.74	30.32	34.29	29.70	33.32	30.56	30.18	30.63
CaO	14.38	17.79	16.71	15.17	17.33	13.83	18.51	12.36	17.82	15.05	15.08	15.29
Na_2O	3.10	1.09	1.75	2.92	1.56	3.31	1.04	4.00	1.31	2.89	2.78	2.65
K_2O	0.11	0.05	0.05	0.05	0.02	0.04	0.02	0.05	0.01	0.04	0.06	0.05
Total	98.06	99.01	98.73	97.78	99.18	98.69	99.93	99.81	98.97	98.04	97.72	98.19
Ab	27.4	10.0	15.9	25.7	14.0	30.2	9.2	36.8	11.7	25.8	24.9	23.6
An	71.9	89.7	83.8	74.0	85.9	69.6	90.7	62.9	88.2	74.0	74.8	76.1
Or	0.7	0.3	0.3	0.3	0.1	0.2	0.1	0.3	0.1	0.2	0.3	0.3

Note: Analysts: R.F. Symes and J. C. Leverton (by electron microprobe).

[a]Average of three.

[b]Average of two.

[c]Average of four.

Uranium Concentrations in Oceanic Tholeiites (μg/g U)

Sample (Interval in cm)	Overall abundance	Glass and mesostasis	Palagonite	Other
250A-26-6, 58	0.50	1.2-6.0		
254-35-1, 118	0.094	0.1-0.6-7.7		Bowl-
256-10-2, 87	0.27	1.0-38	0.05-0.10	ingsite
256-10-4, 131	0.28	0.5-1.0	0.10-0.15	0.20-
257-17-4, 122	0.045	0.07-0.3	0.002-0.005	0.25
257-17-5, 78	0.039	0.4-1.5	0.002-0.01	

basalt series in having high Al^2O^3, relatively high K^2O, and enrichment in certain trace elements.

Site 251

This basalt from the Southwest Branch of the Indian Ocean Ridge is, as might be expected, the most typical oceanic tholeiite of those investigated. It possesses few, if any, unusual characteristics other than its very coarse subophitic texture with embayed plagioclase laths indicating that they formed after the pyroxene.

Sites 253 and 254

The two Ninetyeast Ridge Sites yielded basalts which, like those from Leg 22, show affinities with mantle plume "hot spot" rocks (Frey et al., this volume, Chapter 23). Chemically they are notable for the high MgO of the talc-rich Site 253 "basement", resulting in a (recalculated) olivine-normative composition, and its low CaO and very low Na_2O. The rock is highly altered, as is the lower of the olivine-normative Site 254 rocks, which contain even less CaO. It is possible that the altered Site 254 rocks were, when fresh, quartz-normative; the loss in SiO_2 resulting from alteration may have a greater effect than the oxidation of the iron.

Site 256

Both the Wharton Basin basalt suites show unusual characteristics, including the fact that two holes from the same geomorphological feature, presumably derived from the same spreading ridge, could yield such chemically different rock types. Both are among the most quartz-normative of all analyzed oceanic tholeiites. The first (Site 256) has very high total iron and TiO_2 (and low Al_2O_3 and SiO_2) and is abnormally magnesium- (and nickel-) depleted. The three analyses of these rocks are remarkable for their homogeneity in every respect. The group shows slight normal (but extreme) iron-enrichment upwards but abnormal calcium-enrichment upwards (Figure 15). These rocks are chemically remarkably similar to the last analysis in Table 9 of Shido et al. (1971, p. 265), and, like the FETI basalt from Site 32, eastern Pacific Ocean (Melson, 1973), show extreme fractionation.

Site 257

The Site 257 basalts are also highly quartz-normative, but chemically are fairly typical "primitive" ocean-floor tholeiites. They do not share the iron- and titanium-enrichment seen at Site 256. Their pyroxene and plagioclase compositions are extreme: the phenocrysts, endiopside and bytownite (An_{87}), the groundmass, low-Fe augite and bytownite (An_{73}). The suite shows normal calcium-depletion upwards but strong, abnormal, iron-depletion upwards also (Figures 16 and 17). There is slight titanium-enrichment upward.

If it is assumed that the Wharton Basin basalts, especially at Site 257, were emplaced as a series of concordant flows, with up to 100 m.y. separating 58 meters of basalt, and that crystallization fractionation has resulted in differentiation of the magma, a model is

required to explain the mechanism. This requires normal sequential extrusion, with no question of overturn or other form of inversion of the layered structure. The "primitive" nature of the (endiopside) pyroxene phenocrysts and the highly calcic nature of the (bytownite) plagioclase phenocrysts suggest a derivation from deep in the crust (?layer 3) or the upper mantle. Normal fractionation in the phenocryst-groundmass sequence of both minerals, and normal (Ca→(Na + K)) differentiation of the magma has to be reconciled with Fe→Mg differentiation. The latter, and the high quartz-normativeness of the Wharton Basin basalts, suggest high-level production of a silica undersaturated liquid (Green and Ringwood, 1967). Although the evidence is very limited, the indications at Site 256 are that (Na+K)→Ca and Mg→Fe differentiation occurred: in view of the limited data available, this phenomenon calls for no further comment. In the absence of a relatively simple mineralogical explanation for the unexpectedly reversed Mg-Fe fractionation, such as could be provided by titanium-magnetite-rich basalt formed early under high-oxygen fugacity (Shido et al., 1971), it is suggested that partial melting of a low-melting, nonrefractory, iron-rich portion of the mantle, possibly itself already fractionated with respect to iron and magnesium, may have taken place. This could have been achieved by convective overturn or by selective partial melting of the upper (but high temperature) regions of the mantle (pyrolite) near the center of a mid-ocean ridge (see Aumento, 1967, 1968; Gast, 1968, p. 1083). Alternatively, an olivine-tholeiitic magma rising slowly towards a low-pressure area might have time to fractionate as it rose (Hekinian and Aumento, 1973). Miyashiro et al. (1969) suggested that a primary magma with the composition of low-alumina olivine tholeiite (Green and Ringwood, 1967) would produce a high-alumina abyssal tholeiite magma, precipitating plagioclase phenocrysts, after differentiation at a depth of about 30 km. Because of their structural position near the centers of ocean ridges, strongly quartz-normative abyssal tholeiites are virtually unobtainable by dredging along ridge flank slopes: possibly they are not extruded at the surface, even in the axial regions of ridges, and deep drilling is required to reach them after sea-floor spreading has carried them away from the ridge. Aumento (1968) showed that dredged basalts from the floor of the Median Rift Valley, while tholeiitic, with low alkali and normative olivine content, are still olivine tholeiites, and not quartz tholeiites as are many of the drilled basalts. This could explain the rarity of the quartz tholeiites, and also the fact that abnormal Fe→Mg fractionation of rocks which subsequently undergo normal Ca→(Na + K) fractionation, and normal pyroxene and plagioclase phenocryst→groundmass trends, have hitherto not been detected. It has been shown experimentally (Yoder and Tilley, 1962) that alkali basalts cannot be derived from tholeiitic basalt magma by fractional crystallization, as suggested by Engel, Engel, and Havens (1965). Possibly an oversaturated liquid can be derived from an undersaturated one.

The problem is complicated by the fact that the relative simplicity of the North Atlantic Ocean structure, with a single Ridge consisting of Median Rift Valley and flank mountains, is not repeated in the Indian Ocean. Here, out of six holes drilled into a basalt basement on Leg 26, only one (Site 251) is comparable with the Mid-Atlantic Ridge and a further two or three with normal sea-floor basalt (Sites ?250, 256, 257). However, of the latter three sites, the high olivine-normative nature of the first and the remarkable chemical differences between the last two suggest that certainly not all, and possibly none, of the three are in any way typical.

ACKNOWLEDGMENTS

The author is grateful to Dr. A. C. Bishop for critically reviewing the manuscript and making many helpful suggestions. J. V. Brown took the photomicrographs and Mrs. R. J. Walker drew the figures. Miss Eva Fejer and L. R. Johnson did the X-ray identifications.

REFERENCES

Aumento, F., 1967. Magmatic evolution on the Mid-Atlantic Ridge: Earth Planet. Sci. Lett., v. 2, p. 225.

———, 1968. The Mid-Atlantic Ridge near 45°N. II. Basalts from the area of Confederation Peak: Canadian J. Earth Sci., v. 5, p. 1.

Bence, A. E., Papike, J. J., Chandrasekharam, D., and Cameron, M., 1973a. Petrology of basalts from Leg 17 of the Deep Sea Drilling Project: Central Pacific Basin, (Abstract): EOS, v. 54, p. 998.

Bence, A. E., Papike, J. J., Chandrasekharam, D., Cameron, M., and Camenisch, S., 1973b. Petrology of basalts from Leg 15 of the Deep Sea Drilling Project: the central Caribbean, (Abstract): EOS, v. 54, p. 998.

Berzurkov, P. L., Krylov, A. Y. and Chernysheva, V. I., 1966. Petrography and absolute age of the Indian Ocean floor basalts: Okeanologiya, Akad. Nauk SSSR, v. 6, p. 261.

Bunce, E. T. and Fisher, R. L., in preparation. Introduction. *In* Fisher, R. L., Bunce, E. T., et al., Initial Reports of the Deep Sea Drilling Project, Volume 24: Washington (U.S. Government Printing Office).

Cann, J. R., 1969. Spilites from the Carlsberg Ridge, Indian Ocean: J. Petrol., v. 10, p. 1.

———, 1970. Rb, Sr, Y, Zr and Nb in some ocean floor basaltic rocks: Earth Planet. Sci. Lett., v. 10, p. 7.

———, 1971. Major element variations in ocean-floor basalts: Roy. Soc. London Phil. Trans., Ser. A, v. 268, p. 495.

Chayes, F., 1972. Silica saturation in Cenozoic basalt: Roy. Soc. London Phil. Trans., Ser. A, v. 271, p. 285.

Dymond, J., 1973. K-Ar dating of basalt from DSDP 163: Leg 16, Deep Sea Drilling Project. *In* van Andel, T. H., Heath, G. R., et al., Initial Reports of the Deep Sea Drilling Project, Volume 16: Washington (U.S. Government Printing Office), p. 651.

Engel, A. E. J., Engel, C. G. and Havens, R. G., 1965. Chemical characteristics of oceanic basalts and the upper mantle: Geol. Soc. Am. Bull., v. 76, p. 719.

Engel, C. G. and Fisher, R. L., 1969. Lherzolite, anorthosite, gabbro, and basalt dredged from the Mid-Indian Ocean Ridge: Science, v. 166, p. 1136.

Engel, C. G., Fisher, R. L., and Engel, A. E. J., 1965. Igneous rocks of the Indian Ocean floor: Science, v. 150, p. 605.

Erlank, A. J. and Reid, D. L., in presss. Geochemistry, mineralogy and petrology of basalts, Leg 25, Deep Sea Drilling Project. *In* Simpson, E. S. W., Schlich, R., et al., Initial Reports of the Deep Sea Drilling Project, Volume 25: Washington (U.S. Government Printing Office).

Fisher, R. L., Engel, C. G., and Hilde, T. W. C., 1968. Basalts dredged from the Amirante Ridge, western Indian Ocean: Deep-Sea Res., v. 15, p. 521.

Freisen, W. B., 1973. Igneous and metamorphic rocks recovered by the Deep Sea Drilling Project, Legs 1-31, (Abstract): EOS, v. 54, p. 983.
Gast, P. W., 1968. Trace element fractionation and the origin of tholeiitic and alkaline magma types. Geochim. Cosmochim. Acta, v. 32, p. 1057.
Green, D. H. and Ringwood, A. E., 1967. The genesis of basaltic magmas: Contrib. Mineral. Petrol., v. 15, p. 103.
Hart, R., 1970. Chemical exchange between sea water and deep ocean basalts: Earth Planet. Sci. Lett., v. 9, p. 269.
Hart, S. R., 1969. K, Rb, Cs contents and K/Rb, K/Cs ratios of fresh and altered submarine basalts: Earth Planet. Sci. Lett., v. 6, p. 295.
———, 1971. K, Rb, Cs, Sr, and Ba contents and Sr isotope ratios of ocean floor basalts: Roy. Soc. London Phil. Trans. Series, A, v. 268, p. 573.
Hart, S. R. and Nalwalk, A. J., 1970. K, Rb, Cs and Sr relationships in submarine basalts from the Puerto Rico Trench: Geochim. Cosmochim. Acta, v. 34, p. 145.
Hart, S. R., Brooks, C., Krogh, T. E., Davis, G. L. and Nava, D., 1970. Ancient and modern volcanic rocks: a trace element model: Earth Planet. Sci. Lett., v. 10, p. 17.
Hekinian, R., 1968. Rocks from the Mid-Oceanic Ridge in the Indian Ocean: Deep-Sea Res., v. 15, p. 195.
———, 1973. Petrology of rocks from the northeastern Indian Ocean basins and the Ninetyeast Ridge, (Abstract): EOS, v. 54, p. 1006.
———, 1974a. Petrology of igneous rocks from Leg 22 in the northeastern Indian Ocean. *In* von der Borch, C. C., Sclater, J. G., et al., Initial Reports of the Deep Sea Drilling Project, Volume 22: Washington (U.S. Government Printing Office).
———, 1974b. Petrology of the Ninetyeast Ridge (Indian Ocean) compared to other aseismic ridges: Contrib. Mineral. Petrol., v. 43, p. 125.
Hekinian, R. and Aumento, F., 1973. Rocks from the Gibbs fracture zone and the Minia seamount near 53°N in the Atlantic Ocean: Marine Geol., v. 14, p. 47.
Hendricks, S. B. and Ross, C. S., 1941. Chemical composition and genesis of glauconite and celadonite: Am. Mineral, v. 26, p. 683.
Kay, R., Hubbard, N. J., and Gast, P. W., 1970. Chemical characteristics and origin of oceanic ridge volcanic rocks: J. Geophys. Res., v. 75, p. 1585.
Kempe, D. R. C., 1973a. Basalts from the southern Indian Ocean: DSDP Leg 26, (Abstract): EOS, v. 54, p. 1008.
———, 1973b. Rocks from Antarctica: the *Discovery* collection: British Museum (Nat. Hist.) Bull., Mineral., v. 2, p. 335.
Kempe, D. R. C. and Schilling, J.-G., 1974. Discovery Tablemount basalt: petrology and geochemistry: Contrib. Mineral. Petrol., v. 44, p. 101.
Korzhinsky, D. S., 1962. Spilite problem and the transvapourization hypothesis in the light of new oceanological and vulcanological data: Bull. Acad. Sci. URSS Ser. Geol. no. 9, p. 12.
Lacroix, M. A., 1916. Sur le minéral colorant le plasma de Madagascar et sur la céladonite. Soc. Franc. Mineral. Crist. Bull., v. 39, p. 90.
Mason, P. K., Frost, M. T. and Reed, S. J. B., 1969. BM-IC-NPL computer program for calculating corrections in quantitative X-ray microanalysis: Nat. Phys. Lab. (U.K.), Report 1.
Melson, W. G., 1973. Basaltic glasses from the Deep Sea Drilling Project, chemical characteristics, compositions of alteration products, and fission track "ages", (Abstract): EOS, v. 54, p. 1011.
Miyashiro, A., Shido, F., and Ewing, M., 1969. Diversity and origin of abyssal tholeiite from the Mid-Atlantic Ridge near 24° and 30°N latitude: Contrib. Mineral. Petrol., v. 23, p. 38.
———, 1970. Crystallization and differentiation in abyssal tholeiites and gabbros from mid-oceanic ridges: Earth Planet. Sci. Lett., v. 7, p. 361.
Muir, I. D. and Tilley, C. E., 1964. Basalts from the northern part of the rift zone of the Mid-Atlantic Ridge: J. Petrol., v. 5, p. 409.
———, 1966. Basalts from the northern part of the Mid-Atlantic Ridge. II. The *Atlantis* collections near 30°N: J. Petrol., v. 7, p. 193.
Muir, I. D., Tilley, C. E. and Scoon, J. H., 1957. Contribution to the petrology of Hawaiian basalts. 1. The picrite basalts of Kilauea: Am. J. Sci., v. 225, p. 241.
Pearce, J. A. and Cann., J. R., 1973. Tectonic setting of basic volcanic rocks determined using trace element analyses: Earth Planet. Sci. Lett., v. 19, p. 290.
Rhodes, J. M., 1973. Major and trace element chemistry of basalts from Leg 9 of the Deep Sea Drilling Project, (Abstract): EOS, v. 54, p. 1014.
Ross, C. S., Foster, M. D., and Meyers, A. T., 1954. Origin of dunites and of olivine-rich inclusions in basaltic rocks: Am. Mineral., v. 39, p. 693.
Sheppard, R. A., Gude, A. J., III, and Griffin, J. J., 1970. Chemical composition and physical properties of phillipsite from the Pacific and Indian Oceans: Am. Mineral., v. 55, p. 2053.
Shido, F., Miyashiro, A., and Ewing, M., 1971. Crystallization of abyssal tholeiites: Contrib. Mineral. Petrol., v. 31, p. 251.
Subbarao, K. V. and Hedge, C. E., 1973. K, Rb, Sr and $^{87}Sr/^{86}Sr$ in rocks from the Mid-Indian Oceanic Ridge: Earth Planet. Sci. Lett., v. 18, p. 223.
Sweatman, T. R. and Long, J. V. P., 1969. Quantitative electron-probe microanalysis of rock-forming minerals: J. Petrol., v. 10, p. 332.
Thompson, G., Shido, F. and Miyashiro, A., 1972. Trace element distributions in fractionated oceanic basalts. Chem. Geol., v. 9, p. 89.
Yeats, R. S., Forbes, W. C., Heath, G. R., and Scheidegger, K. F., 1973. Petrology and geochemistry of DSDP Leg 16 basalts, eastern equatorial Pacific. *In* van Andel, T. H., Heath, G. R., et al., Initial Reports of the Deep Sea Drilling Project, Volume 16: Washington (U.S. Government Printing Office), p. 617.
Yoder, H. S., Jr. and Tilley, C. E., 1962. Origin of basalt magmas: an experimental study of natural and synthetic rock systems: J. Petrol., v. 3, p. 342.

APPENDIX A
URANIUM DISTRIBUTION AND ABUNDANCE IN SIX BASALTS FROM SITES 250, 254, 256, 257

J. D. Kleeman, Department of Geology,
University of New England, Armidale, New South Wales, Australia

Lexan plastic prints (Kleeman and Lovering, 1967, Kleeman, 1973) were taken by registering fission tracks in a plastic sheet during a thermal neutron irradiation. Subsequently the tracks were made visible to an optical microscope by etching with NaOH solution. Fission tracks were observed using two procedures.

1) One hundred randomly placed fields of view were counted to provide an overall estimate of uranium concentration in the rock section.

2) The distribution of uranium was correlated with the phases producing various densities of fission tracks.

RESULTS

Uranium Abundance of the Basalts

The overall uranium concentrations, shown below, range from 0.04 to 0.5 μg/g U. The upper end of this range is higher than those usually associated with oceanic tholeiites (0.05-0.16 μg/g, Tatsumoto et al., 1965).

Distribution of Uranium

The major crystalline phases, pyroxene and plagioclase, have low uranium concentrations. Since grain size is not large, the detection limit is relatively high, as large areas cannot be counted. Both phases have <0.005 μg/g U. Grain boundaries have generally little uranium, much less than one order of magnitude more than that in plagioclase and pyroxene. This asserts the general freshness of the rocks, and absence of any general mobilization of uranium after crystallization.

Most of the uranium is concentrated in late crystallizing phases, either glass or derivatives of it, in amounts shown above. In places, spots of relatively high uranium concentrations suggest phases within these areas, but none were identified.

One of the rocks contains patches of bowlingite (Site 254) after olivine, also uranium bearing. The others have various amounts of palagonite, apparently pseudomorphing olivine and less commonly vesicle filling. These patches are distinguished from mesostasis patches by their more massive appearance, quite distinctive on the polished surface, and absence of any iron-oxide phase. The palagonite is comparatively impoverished in uranium, more or less in proportion to the overall amounts of uranium in the rock. Like bowlingite, it appears to be formed after the initial crystallization of the rock, and the uranium in it is either derived from the areas of mesostasis or derived from outside the rock. Uranium in these phases is not the major contributor to the overall content of the rocks.

The present abundances, therefore, seem to be a first order reflection of the uranium concentration of the freshly crystallized rocks.

ACKNOWLEDGMENTS

This work was supported by the Australian Research Grants Committee; the thermal neutron irradiations were financed by the Australian Institute for Nuclear Science and Engineering, and performed at the Australian Atomic Energy Commission Research Establishment.

REFERENCES

Kleeman, J. D., 1973. The role of lithium and boron in producing Lexan plastic prints: Geochim. Cosmochim. Acta, v. 37, p. 1321.

Kleeman, J. D. and Lovering, J. F., 1967. Uranium distribution in rocks by fission track registration in Lexan plastic: Science, v. 156, p. 512.

Tatsumoto, M., Hedge, C. E., and Engel, A. E. J., 1965. Potassium, strontium, thorium, and uranium and the ratio of Sr-87 to Sr-86 in oceanic tholeiitic basalt: Science, v. 150, p. 886.

PLATE 1

Figure 1 Photomicrograph of variolitic basalt, Mozambique Basin (DSDP 250A-25-1, 110 cm). Plane polarized light (Ppl), ×13.

Figure 2 Photomicrograph of variolitic basalt, H.E.M.S. *Mahabiss,* Station 133 (1°25′54″S, 66°34′12″E). Ppl, ×13.

Figure 3 Photomicrograph of subophitic olivine basalt, Mozambique Basin (DSDP 250A-25-1, 135 cm). Ppl, ×13.

Figure 4 Photomicrograph of subophitic olivine basalt, Mozambique Basin (DSDP 250A-26-6, 46 cm). Crossed polars (Cp), ×13.

Figure 5 Photomicrograph of glassy basalt. Southwest Branch, Indian Ocean Ridge (DSDP 251A-29-1, 161 cm). Ppl, ×13.

Figure 6 Photomicrograph of subophitic basalt, Southwest Branch, Indian Ocean Ridge (DSDP 251A-31-4, 30 cm). Cp, ×13.

PLATE 1

1

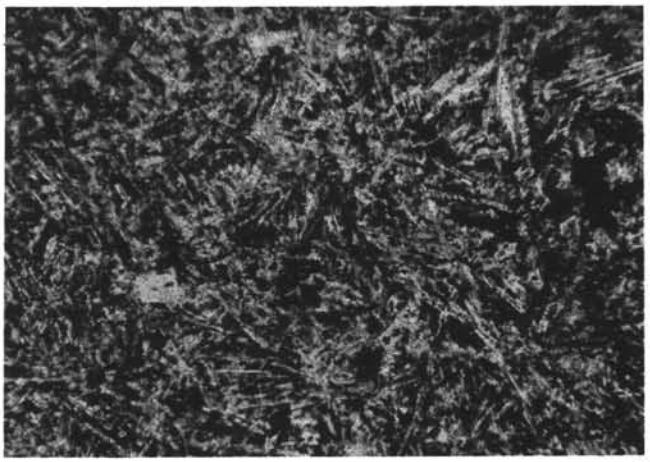

2

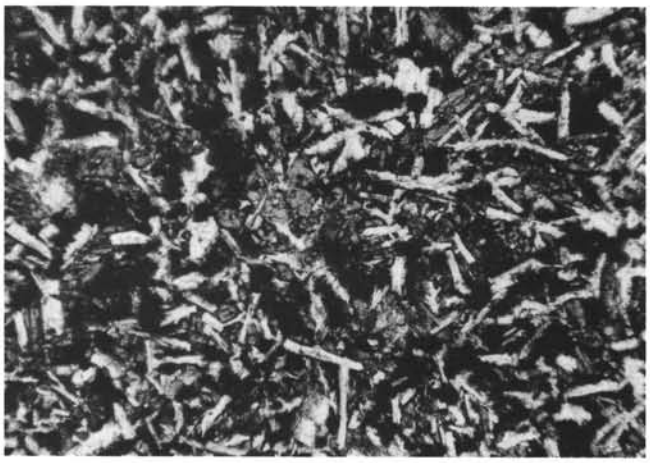

3

4

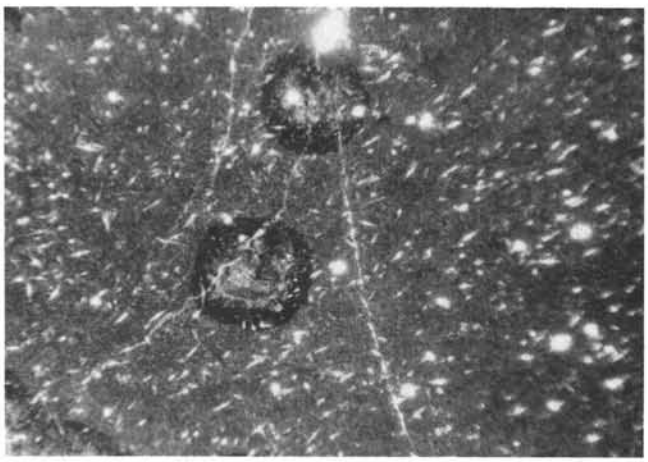

5

6

PLATE 2

Figure 1 — Photomicrograph of coarse subophitic basalt, Southwest Branch, Indian Ocean Ridge (DSDP 251A-31-5, 100 cm). Note embayed plagioclase laths, formed around pre-existing pyroxene. Cp, ×13.

Figure 2 — Photomicrograph of scoriaceous olivine basalt flow, Ninetyeast Ridge (DSDP 253-24-1, 93 cm). Ppl, ×13.

Figure 3 — Photomicrograph of olivine basaltic glass, Ninetyeast Ridge (DSDP 253-24-1, 109 cm). Note vesicles, sparse fresh olivines, and minute rhombic plagioclase crystals. Ppl, ×21.

Figure 4 — Photomicrograph of olivine basaltic glass, DODO 113 (23°16′S, 74°59′E). Ppl, ×13.

Figures 5, 6 — Photomicrographs of fairly altered picritic basalt, Ninetyeast Ridge (DSDP 253-58-1, 3 cm and 58-CC). Note olivine crystals pseudomorphed by talc and serpentine. Cp, ×13.

PLATE 2

1

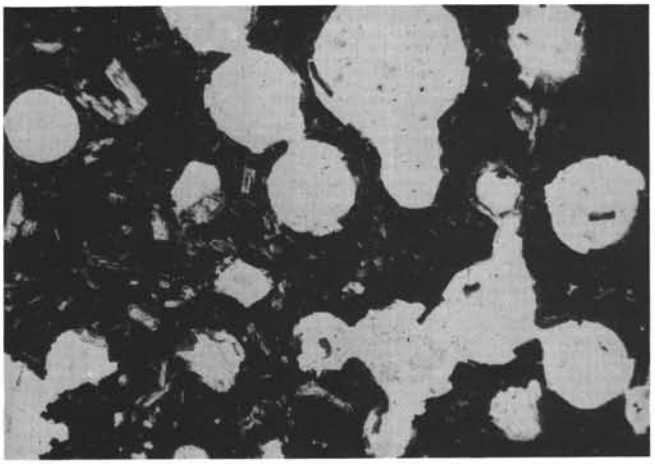

2

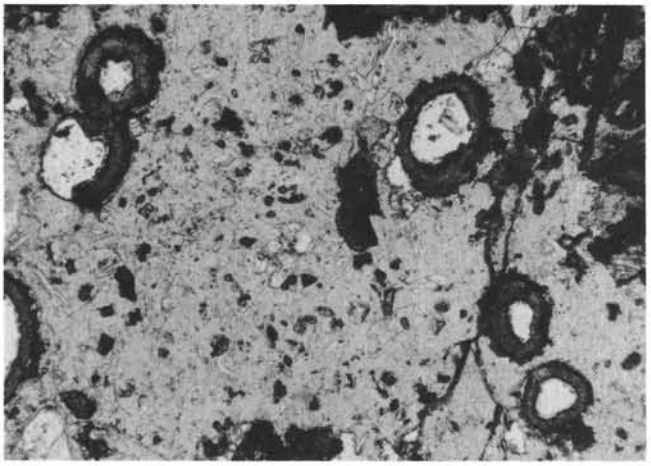

3

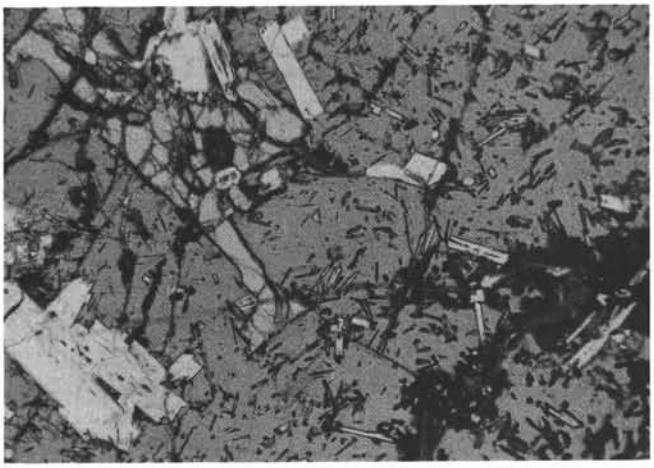

4

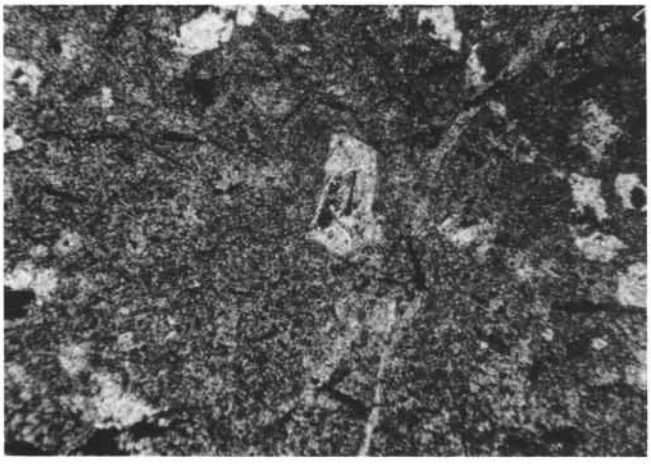

5

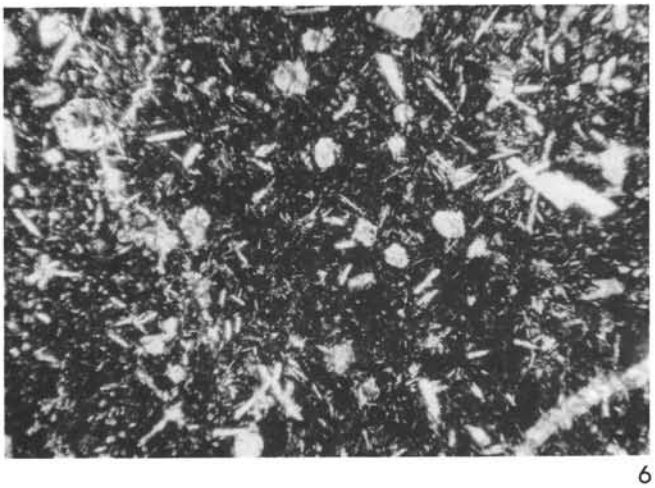

6

PLATE 3

Figure 1 Photomicrograph of hyalo-ophitic basalt, Ninetyeast Ridge (DSDP 254-31-1, 110 cm). Cp, ×13.

Figure 2 Photomicrograph of altered amygdaloidal basalt, Ninetyeast Ridge (DSDP 254-36-1, 60 cm). Cp, ×13.

Figure 3 Photomicrograph of altered hyalo-ophitic basalt, Ninetyeast Ridge (DSDP 254-36-3, 96 cm). Cp, ×13.

Figure 4 Photomicrograph of totally altered basalt (smectite), Ninetyeast Ridge (DSDP 254-38-1, 116 cm). Cp, ×13.

Figure 5 Photomicrograph of hyalo-ophitic basalt with calcite and celadonite vein, Wharton Basin (DSDP 256-9-2, 51 cm). Celadonite can be seen to be replacing all the minerals in the rock, including plagioclase. Ppl, ×13.

Figure 6 Photomicrograph of subophitic basalt, Wharton Basin (DSDP 256-10-2, 87 cm). Cp, ×13.

PLATE 3

1

2

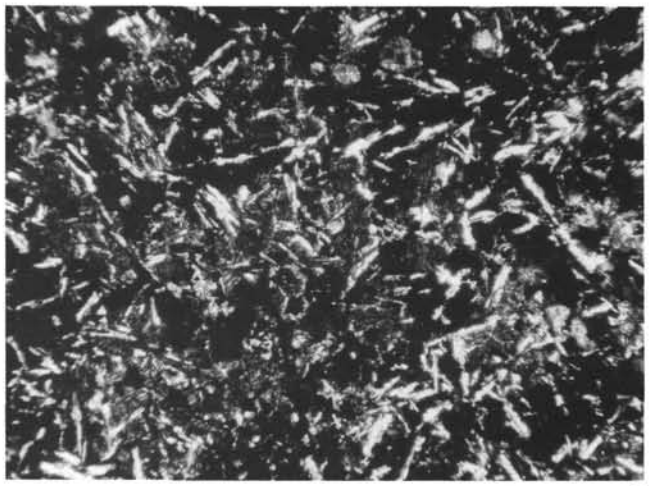

3

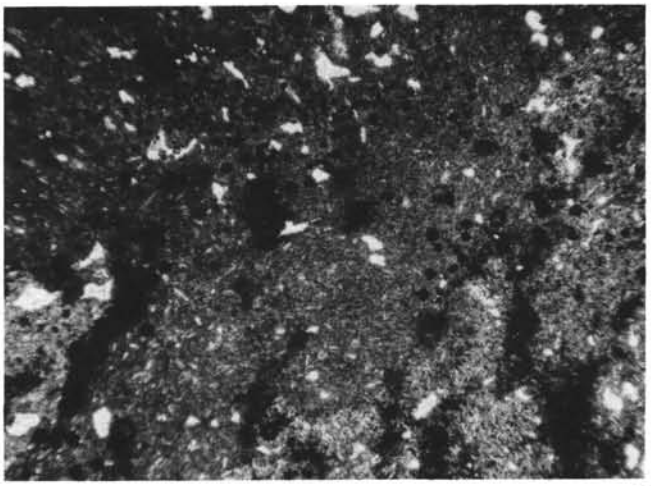

4

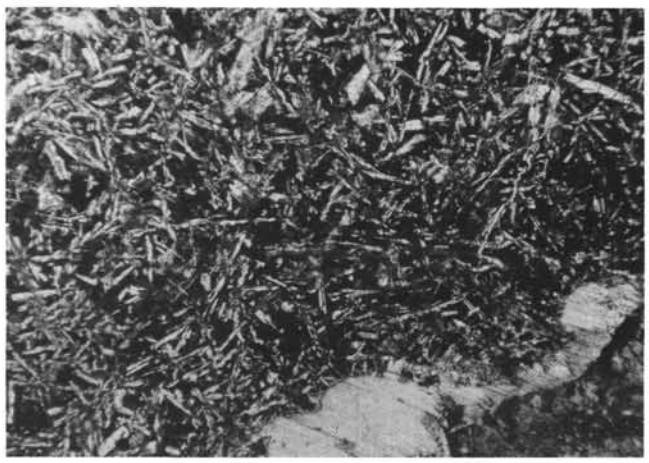

5

6

PLATE 4

Figure 1 Photomicrograph of variolitic glassy basalt, Wharton Basin (DSDP 256-10-4, 87 cm). Note large rhombic plagioclase. Ppl, ×13.

Figure 2 Photomicrograph of hyalo-ophitic basalt, Wharton Basin (DSDP 256-11-3, 110 cm). Cp, ×13.

Figure 3 Photomicrograph of vesicular hyalo-ophitic basalt, Wharton Basin (DSDP 257-11-2, 27 cm). The vesicles are filled with smectite, calcite, and some celadonite. Ppl, ×13.

Figure 4 Photomicrograph of vesicular hyalo-ophitic basalt, Wharton Basin (DSDP 257-11-3, 29 cm). The vesicles are variously filled, as in Figure 3. Cp, ×13.

Figure 5 Photomicrograph of vesicular glassy basalt, Wharton Basin (DSDP 257-13-2, 80 cm). The vesicles are filled with vivid green celadonite. Ppl, ×13.

Figure 6 Photomicrograph of vesicular hyalo-ophitic basalt, Wharton Basin (DSDP 257-13-3, 10 cm). The vesicles are filled with calcite. Ppl, ×13.

PLATE 4

1

2

3

4

5

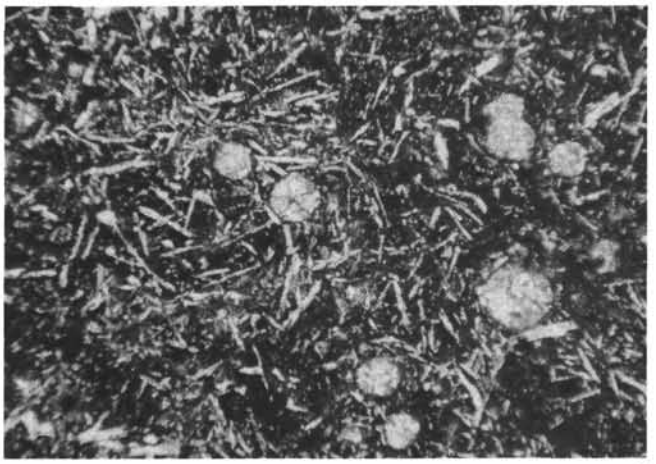

6

PLATE 5

Figure 1 Photomicrograph of variolitic basalt with celadonite vein, Wharton Basin (DSDP 257-14-4, 22 cm). Ppl, ×13.

Figure 2 Photomicrograph of porphyritic subophitic basalt, Wharton Basin (DSDP 257-14-4, 125 cm). Cp, ×13.

Figure 3 Photomicrograph of subophitic basalt, Wharton Basin (DSDP 257-151B, 126 cm). Cp, ×13.

Figure 4 Photomicrograph of fine-grained subophitic basalt, Wharton Basin (DSDP 257-15-2, 38 cm). Note embayed plagioclase laths, formed around pre-existing pyroxene. Cp, ×34.

Figure 5 Photomicrograph of porphyritic subvariolitic basalt, Wharton Basin (DSDP 257-16-2, 100 cm). Cp, ×13.

Figure 6 Photomicrograph of subvariolitic hyalo-ophitic basalt, Wharton Basin (DSDP 257-17-5, 66 cm). Cp, ×13.

PLATE 5

1

2

3

4

5

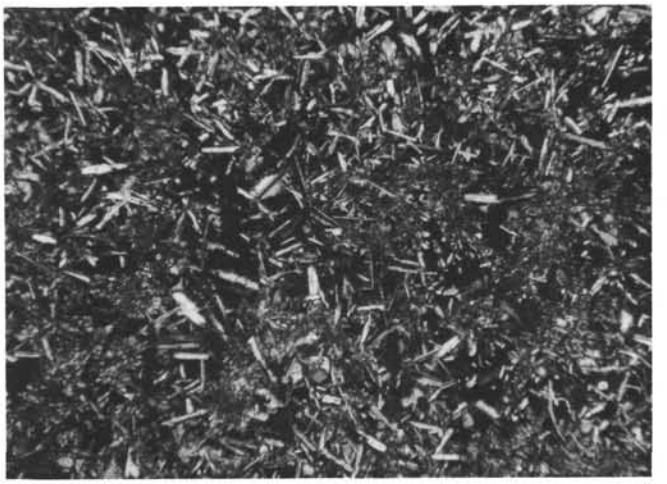

6